Projected Nesterov's Proximal-Gradient Algorithm for Sparse Signal Recovery†

Aleksandar Dogandžić

Electrical and Computer Engineering

IOWA STATE UNIVERSITY

† joint work with Renliang Gu, Ph.D. student

supported by NSF

My Research

General Area

Statistical signal processing

Interests

- Sparse signal reconstruction
  - X-ray CT
- Nondestructive evaluation (NDE)
  - detecting and estimating defects
- High-dimensional statistical inference
  - finding low-dimensional structure in high-dimensional data.

My Research

Applications (present and past)

- NDE,
- biomedicine,
- wireless sensor networks and communications,
- space-time processing for radar.

Terminology and Notation

- soft-thresholding operator for $\boldsymbol{a} = (a_i)_{i=1}^N \in \mathbb{R}^N$:

$$\left[\mathcal{T}_\lambda(\boldsymbol{a})\right]_i = \operatorname{sign}(a_i)\max\left(|a_i| - \lambda, 0\right);$$

- "$\succeq$" is the elementwise version of "$\geq$";
- proximal operator for function $r(\boldsymbol{x})$ scaled by λ:

$$\operatorname{prox}_{\lambda r}\boldsymbol{a} = \arg\min_{\boldsymbol{x}} \tfrac{1}{2}\|\boldsymbol{x} - \boldsymbol{a}\|_2^2 + \lambda r(\boldsymbol{x}).$$

- ε-subgradient (Rockafellar 1970, Sec. 23):

$$\partial_\varepsilon r(\boldsymbol{x}) \triangleq \left\{\boldsymbol{g} \in \mathbb{R}^p \mid r(\boldsymbol{z}) \geq r(\boldsymbol{x}) + (\boldsymbol{z} - \boldsymbol{x})^T\boldsymbol{g} - \varepsilon, \forall \boldsymbol{z} \in \mathbb{R}^p\right\}.$$

Introduction

For most natural signals $\boldsymbol{x}$,

$$\#\text{ significant coefficients of } \Psi^T \boldsymbol{x} \ll \text{signal size } p$$

where Ψ is a known *sparsifying dictionary* matrix.

Sparsifying Transforms: Discrete wavelet transform (DWT)

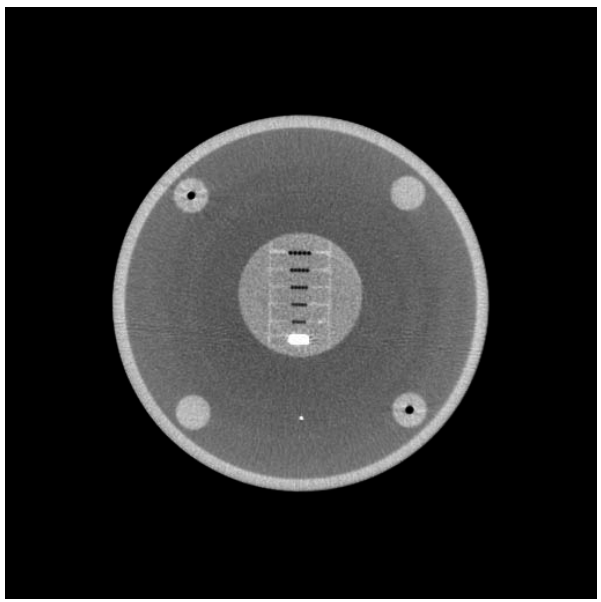

p pixels

transform
$\leftrightarrow$
DWT

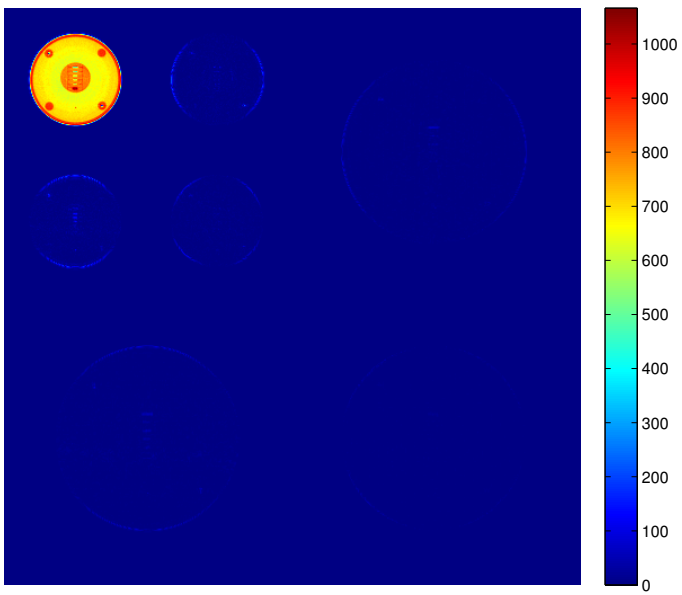

$\#$ significant coeffs $\ll p$

Sparsifying Transforms: Gradient Map, Total Variation

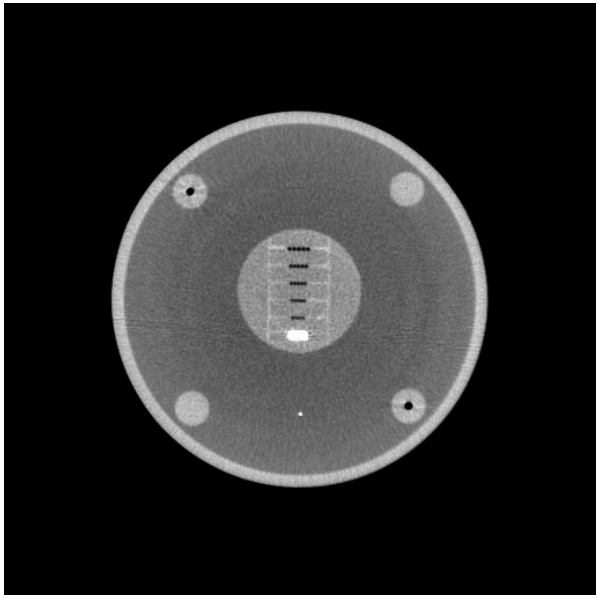

transform
$\leftrightarrow$
gradient map

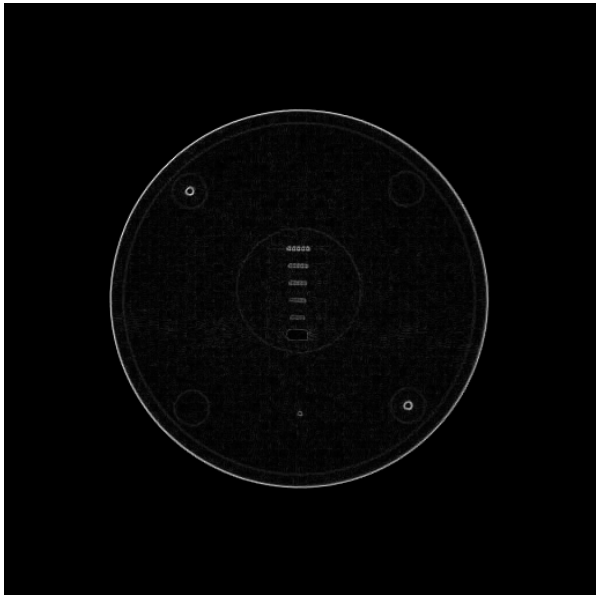

p pixels

$\#$ significant coeffs $\ll p$

Ψ is complex.

Convex-Set Constraint

$$\boldsymbol{x} \in \boldsymbol{C}$$

where $\boldsymbol{C}$ is a nonempty closed convex set.

Example: the nonnegative signal set

$$C = \mathbb{R}_+^p$$

is of significant practical interest and applicable to X-ray CT, SPECT, PET, and MRI.

Convex-Set Constraint

$$\boldsymbol{x} \in \boldsymbol{C}$$

where $\boldsymbol{C}$ is a nonempty closed convex set.
Example: the nonnegative signal set

$$\boldsymbol{C} = \mathbb{R}_+^{\boldsymbol{p}}$$

is of significant practical interest and applicable to X-ray CT, SPECT, PET, and MRI.

Goal

Sense the significant components of $\Psi^T \boldsymbol{x}$ using a small number of measurements.

Noisy measurement process described by the negative log-likelihood (NLL) $\mathcal{L}(\boldsymbol{x})$.

Penalized NLL

- objective function

$$f(\boldsymbol{x}) = \mathcal{L}(\boldsymbol{x}) + u \underbrace{\left[\rho(\boldsymbol{x}) + \mathbb{I}_C(\boldsymbol{x})\right]}_{r(\boldsymbol{x})}$$

- convex differentiable negative log-likelihood (NLL)
- convex penalty term
  $u > 0$ is a scalar tuning constant
  $C \subseteq \mathrm{cl}\big(\mathrm{dom}\, \mathcal{L}(\boldsymbol{x})\big)$

Penalized NLL

- objective function

$$f(\boldsymbol{x}) = \mathcal{L}(\boldsymbol{x}) + u \underbrace{\left[\rho(\boldsymbol{x}) + \mathbb{I}_C(\boldsymbol{x})\right]}_{r(\boldsymbol{x})}$$

- convex differentiable negative log-likelihood (NLL)
- convex penalty term

$u > 0$ is a scalar tuning constant

$C \subseteq \mathrm{cl}\big(\mathrm{dom}\, \mathcal{L}(\boldsymbol{x})\big)$

Penalized NLL

- objective function

$$f(\boldsymbol{x}) = \mathcal{L}(\boldsymbol{x}) + u \underbrace{\left[\rho(\boldsymbol{x}) + \mathbb{I}_C(\boldsymbol{x})\right]}_{r(\boldsymbol{x})}$$

- convex differentiable negative log-likelihood (NLL)
- convex penalty term

$u > 0$ is a scalar tuning constant

$C \subseteq \mathrm{cl}\big(\mathrm{dom}\, \mathcal{L}(\boldsymbol{x})\big)$

Comment

Our objective function $f(\boldsymbol{x})$ is

- convex
  - has a convex set as minimum (unique if $\mathcal{L}(\boldsymbol{x})$ is strongly convex),
- not differentiable with respect to the signal $\boldsymbol{x}$
  - cannot apply usual gradient- or Newton-type algorithms,
  - need proximal-gradient (PG) schemes.

Typical convex $\rho(\boldsymbol{x})$:

$$\rho(\boldsymbol{x}) = \|\Psi^T \boldsymbol{x}\|_1$$

imposes sparsity of transform signal coefficients $\Psi^T \boldsymbol{x}$.

Goals

Develop a fast algorithm with

- $\mathcal{O}(k^{-2})$ convergence-rate and
- iterate convergence guarantees

for minimizing $f(\boldsymbol{x})$ that

- is general (for a diverse set of NLLs),
- requires minimal tuning, and
- is matrix-free*, a must for solving large-scale problems.

*involves only matrix-vector multiplications implementable using, e.g., function handle in Matlab

Majorizing Function

Define the quadratic approximation of the NLL $\mathcal{L}(\boldsymbol{x})$:

$$Q_\beta\left(\boldsymbol{x} \mid \bar{\boldsymbol{x}}\right) = \mathcal{L}(\bar{\boldsymbol{x}}) + (\boldsymbol{x} - \bar{\boldsymbol{x}})^T \nabla \mathcal{L}(\bar{\boldsymbol{x}}) + \frac{1}{2\beta}\|\boldsymbol{x} - \bar{\boldsymbol{x}}\|_2^2$$

with β chosen so that $Q_\beta\left(\boldsymbol{x} \mid \bar{\boldsymbol{x}}\right)$ majorizes $\mathcal{L}(\boldsymbol{x})$ in the neighborhood of $\boldsymbol{x} = \bar{\boldsymbol{x}}$.

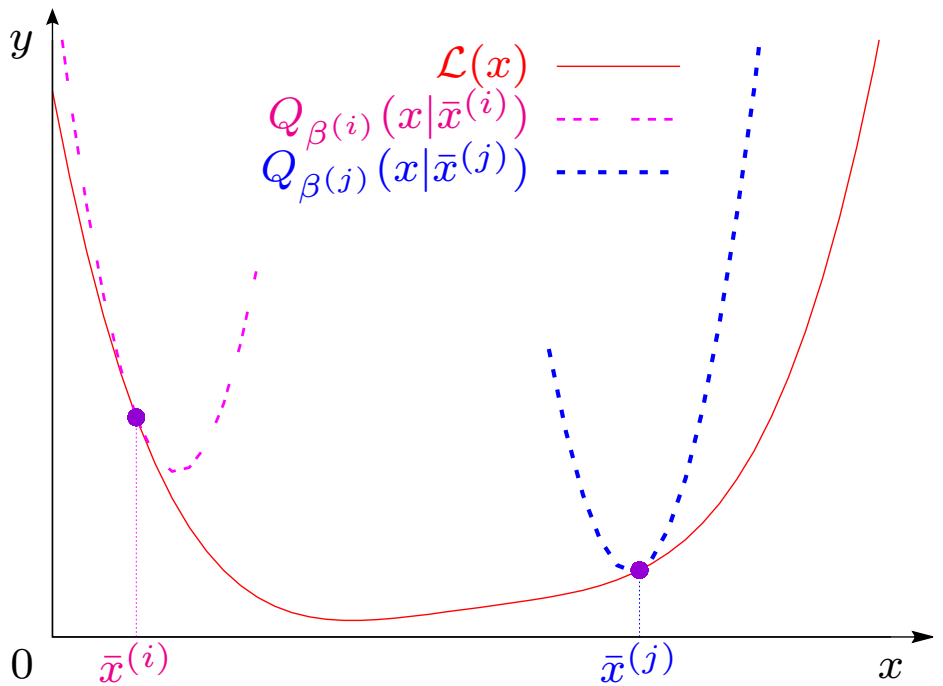

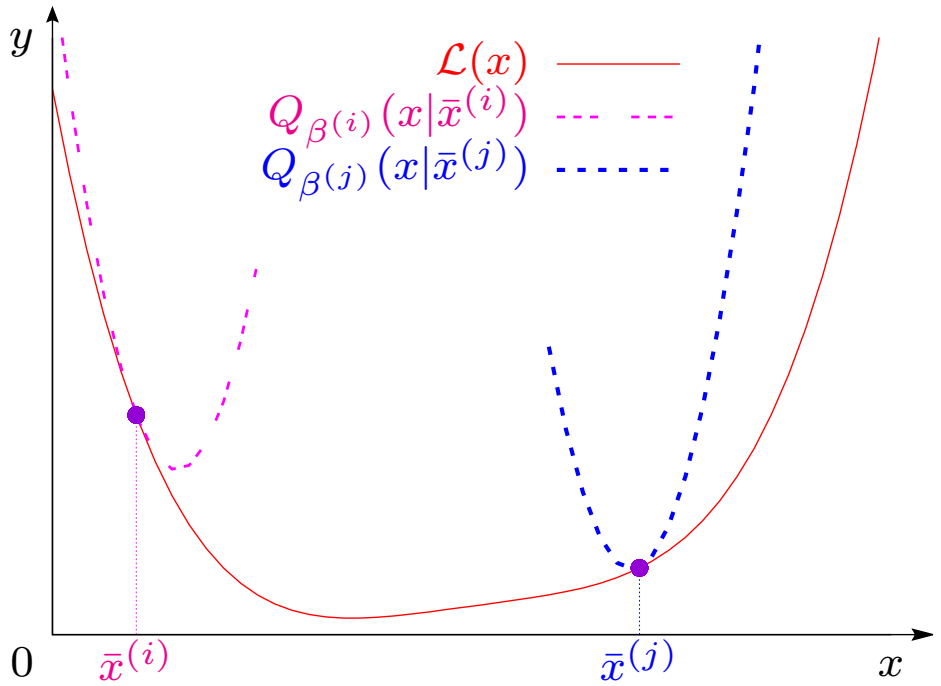

Figure 1: Majorizing function: Impact of β.

No need for strict majorization, sufficient to majorize in the neighborhood of $\bar{x}$ where we wish to move next!

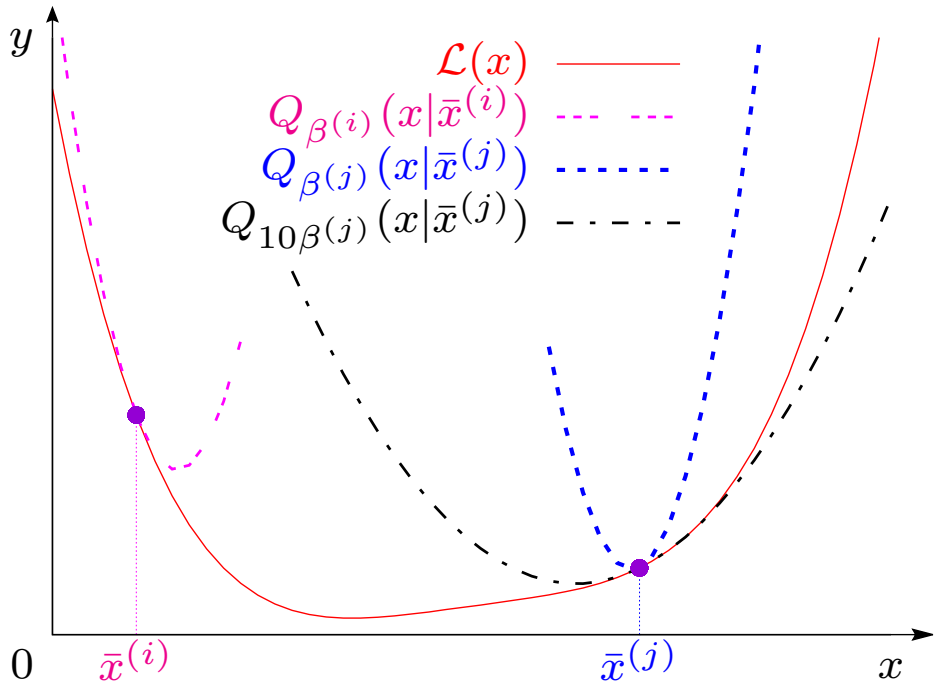

Figure 1: Majorizing function: Impact of β.

No need for strict majorization, sufficient to majorize in the neighborhood of $\bar{\boldsymbol{x}}$ where we wish to move next!

PNPG Method: Iteration i

$$
\begin{aligned}
B^{(i)} &= \beta^{(i-1)}/\beta^{(i)} \\
\theta^{(i)} &= \begin{cases} 1, & i \le 1 \\ \frac{1}{\gamma} + \sqrt{b + B^{(i)}\left(\theta^{(i-1)}\right)^2}, & i > 1 \end{cases} \\
\overline{\boldsymbol{x}}^{(i)} &= P_C\left(\boldsymbol{x}^{(i-1)} + \frac{\theta^{(i-1)} - 1}{\theta^{(i)}}\left(\boldsymbol{x}^{(i-1)} - \boldsymbol{x}^{(i-2)}\right)\right) \qquad \text{accel. step} \\
\boldsymbol{x}^{(i)} &\approx_{\varepsilon^{(i)}} \operatorname{prox}_{\beta^{(i)} ur}\left(\overline{\boldsymbol{x}}^{(i)} - \beta^{(i)} \nabla \mathcal{L}\left(\overline{\boldsymbol{x}}^{(i)}\right)\right) \qquad \text{PG step}
\end{aligned}
$$

where $\beta^{(i)} > 0$ is an *adaptive step size*:

- satisfies

$$\mathcal{L}\left(\boldsymbol{x}^{(i)}\right) \le Q_{\beta^{(i)}}\left(\boldsymbol{x}^{(i)} \mid \overline{\boldsymbol{x}}^{(i)}\right) \qquad \text{majorization condition,}$$

- is as large as possible.

▸ more

PNPG Method: Iteration i

allows general $\operatorname{dom}\mathcal{L}$

$$
\begin{aligned}
B^{(i)} &= \beta^{(i-1)}/\beta^{(i)} \\
\theta^{(i)} &= \begin{cases} i, & i \le 1 \\ \frac{1}{\gamma} + \sqrt{b + B^{(i)}\left(\theta^{(i-1)}\right)^2}, & i > 1 \end{cases} \\
\overline{\boldsymbol{x}}^{(i)} &= P_C\left(\boldsymbol{x}^{(i-1)} + \frac{\theta^{(i-1)} - 1}{\theta^{(i)}}\left(\boldsymbol{x}^{(i-1)} - \boldsymbol{x}^{(i-2)}\right)\right) && \text{accel. step} \\
\boldsymbol{x}^{(i)} &\approx_{\varepsilon^{(i)}} \operatorname{prox}_{\beta^{(i)} ur}\left(\overline{\boldsymbol{x}}^{(i)} - \beta^{(i)}\nabla\mathcal{L}\left(\overline{\boldsymbol{x}}^{(i)}\right)\right) && \text{PG step}
\end{aligned}
$$

where $\beta^{(i)} > 0$ is an *adaptive step size*:

- satisfies

$$\mathcal{L}\left(\boldsymbol{x}^{(i)}\right) \le Q_{\beta^{(i)}}\left(\boldsymbol{x}^{(i)} \mid \overline{\boldsymbol{x}}^{(i)}\right) \qquad \text{majorization condition,}$$

- is as large as possible.

Momentum Illustration

$$\overline{\boldsymbol{x}}^{(i)} = P_C\Big(\overbrace{\boldsymbol{x}^{(i-1)} + \underbrace{\tfrac{\theta^{(i-1)}-1}{\theta^{(i)}}\big(\boldsymbol{x}^{(i-1)} - \boldsymbol{x}^{(i-2)}\big)}_{\text{momentum term prevents zigzagging}}}^{\widehat{\boldsymbol{x}}^{(i)}}\Big)$$

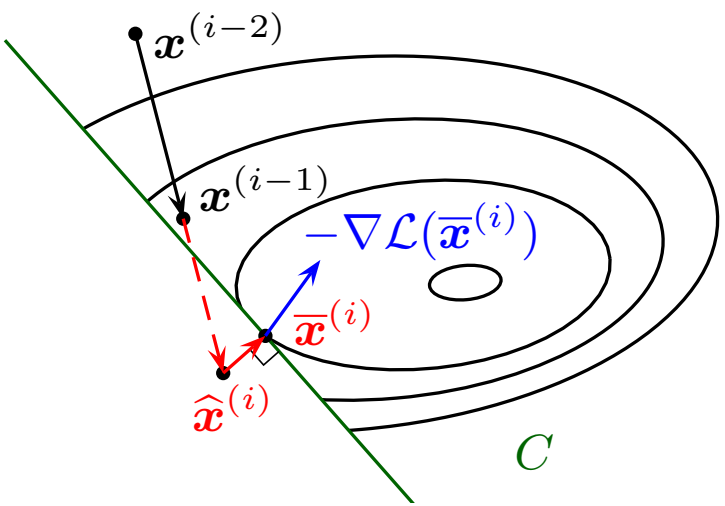

PNPG Method: Iteration i

$$
\begin{aligned}
B^{(i)} &= \beta^{(i-1)}/\beta^{(i)} \\
\theta^{(i)} &= \begin{cases} i, & i \le 1 \\ \frac{1}{\gamma} + \sqrt{b + B^{(i)}\left(\theta^{(i-1)}\right)^2}, & i > 1 \end{cases} \\
\overline{\boldsymbol{x}}^{(i)} &= P_C\left(\boldsymbol{x}^{(i-1)} + \frac{\theta^{(i-1)} - 1}{\theta^{(i)}}\left(\boldsymbol{x}^{(i-1)} - \boldsymbol{x}^{(i-2)}\right)\right) && \text{accel. step} \\
\boldsymbol{x}^{(i)} &\approx_{\varepsilon^{(i)}} \operatorname{prox}_{\beta^{(i)} ur}\left(\overline{\boldsymbol{x}}^{(i)} - \beta^{(i)} \nabla \mathcal{L}\left(\overline{\boldsymbol{x}}^{(i)}\right)\right) && \text{PG step}
\end{aligned}
$$

where $\beta^{(i)} > 0$ is an *adaptive step size*:

- satisfies

needs to hold for $\boldsymbol{x}^{(i)}$, not for all $\boldsymbol{x}$!

$$\mathcal{L}\left(\boldsymbol{x}^{(i)}\right) \le Q_{\beta^{(i)}}\left(\boldsymbol{x}^{(i)} \mid \overline{\boldsymbol{x}}^{(i)}\right) \qquad \text{majorization condition,}$$

$\mathcal{L}(\boldsymbol{x}) \not\le Q_{\beta^{(i)}}(\boldsymbol{x} \mid \overline{\boldsymbol{x}}^{(i)})$ in general, for an arbitrary $\boldsymbol{x}$! ▸ more

PNPG Method: Iteration i

$$
\begin{aligned}
B^{(i)} &= \beta^{(i-1)}/\beta^{(i)} \\
\theta^{(i)} &= \begin{cases} i, & i \le 1 \\ \frac{1}{\gamma} + \sqrt{b + B^{(i)}\left(\theta^{(i-1)}\right)^2}, & i > 1 \end{cases} \\
\bar{\boldsymbol{x}}^{(i)} &= P_C\left(\boldsymbol{x}^{(i-1)} + \frac{\theta^{(i-1)} - 1}{\theta^{(i)}}\left(\boldsymbol{x}^{(i-1)} - \boldsymbol{x}^{(i-2)}\right)\right) && \text{accel. step} \\
\boldsymbol{x}^{(i)} &\approx_{\varepsilon^{(i)}} \operatorname{prox}_{\beta^{(i)} ur}\left(\bar{\boldsymbol{x}}^{(i)} - \beta^{(i)} \nabla \mathcal{L}\left(\bar{\boldsymbol{x}}^{(i)}\right)\right) && \text{PG step}
\end{aligned}
$$

where $\beta^{(i)} > 0$ is an *adaptive step size*:

- satisfies

needs to hold for $\boldsymbol{x}^{(i)}$, not for all $\boldsymbol{x}$!

$$\mathcal{L}\left(\boldsymbol{x}^{(i)}\right) \le Q_{\beta^{(i)}}\left(\boldsymbol{x}^{(i)} \mid \bar{\boldsymbol{x}}^{(i)}\right) \qquad \text{majorization condition,}$$

$\mathcal{L}(\boldsymbol{x}) \not\le Q_{\beta^{(i)}}\left(\boldsymbol{x} \mid \bar{\boldsymbol{x}}^{(i)}\right)$ in general, for an arbitrary $\boldsymbol{x}$!

▸ more

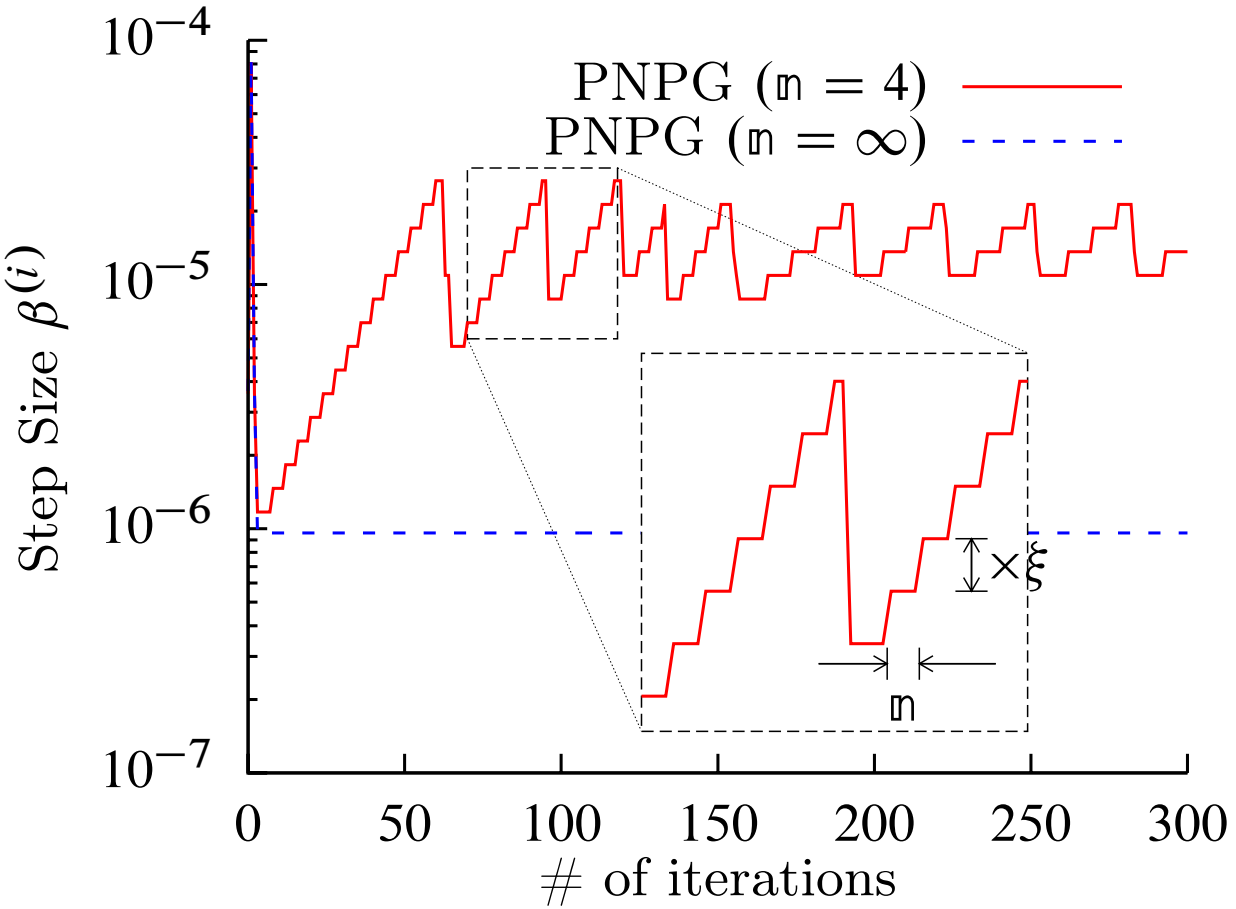

Figure 2: Illustration of step-size selection for Poisson generalized linear model (GLM) with identity link.

Comments on the Extrapolation Term $\theta^{(i)}$

$$\theta^{(i)} = \tfrac{1}{\gamma} + \sqrt{b + B^{(i)}\left(\theta^{(i-1)}\right)^2}, \qquad i \geq 2$$

where

$$\gamma \geq 2, \qquad b \in [0, 1/4]$$

are momentum tuning constants.

- To establish $\mathcal{O}\left(k^{-2}\right)$ convergence of PNPG, need

$$\theta^{(i)} \leq \tfrac{1}{2} + \sqrt{\tfrac{1}{4} + B^{(i)}\left(\theta^{(i-1)}\right)^2}, \qquad i \geq 2.$$

- γ controls the rate of increase of $\theta^{(i)}$.

Comments on the Extrapolation Term $\theta^{(i)}$

$\theta^{(i)}\uparrow$ implies stronger momentum.

Effect of step size

In the "steady state" where $\beta^{(i-1)} = \beta^{(i)}$, $\theta^{(i)}\uparrow$ aproximately linearly with i, with slope $1/\gamma$.
Changes in the step size affect $\theta^{(i)}$:

$\beta^{(i)} < \beta^{(i-1)}$ step size decrease, faster increase of $\theta^{(i)}$,

$\beta^{(i)} > \beta^{(i-1)}$ step size increase, decrease or slower increase of $\theta^{(i)}$ than in the steady state.

Proximal Mapping

To compute

$$\text{prox}_{\lambda r}\, \boldsymbol{a} = \arg\min_{\boldsymbol{x}} \tfrac{1}{2}\|\boldsymbol{x} - \boldsymbol{a}\|_2^2 + \lambda r(\boldsymbol{x})$$

use

- alternating direction method of multipliers (ADMM) for DWT sparsifying transform
  - iterative,
- total-variation (TV)-based denoising method in (Beck and Teboulle 2009b) for TV sparsifying transform
  - iterative.

Inexact PG Steps

$$
\begin{aligned}
B^{(i)} &= \beta^{(i-1)}/\beta^{(i)} \\
\theta^{(i)} &= \begin{cases} i, & i \leq 1 \\ \frac{1}{\gamma} + \sqrt{b + B^{(i)}\left(\theta^{(i-1)}\right)^2}, & i > 1 \end{cases} \\
\bar{\boldsymbol{x}}^{(i)} &= P_C\left(\boldsymbol{x}^{(i-1)} + \frac{\theta^{(i-1)} - 1}{\theta^{(i)}}\left(\boldsymbol{x}^{(i-1)} - \boldsymbol{x}^{(i-2)}\right)\right) \qquad \text{accel. step} \\
\boldsymbol{x}^{(i)} &\approx_{\varepsilon^{(i)}} \operatorname{prox}_{\beta^{(i)} ur}\left(\bar{\boldsymbol{x}}^{(i)} - \beta^{(i)} \nabla \mathcal{L}\left(\bar{\boldsymbol{x}}^{(i)}\right)\right) \qquad \text{PG step}
\end{aligned}
$$

Because of their iterative nature, PG steps are *inexact*: $\varepsilon^{(i)}$ quantifies the precision of the PG step in Iteration i.

▸ more

Remark (Monotonicity)

The projected Nesterov's proximal-gradient (PNPG) iteration with restart is non-increasing:

$$f\left(\boldsymbol{x}^{(i)}\right) \leq f\left(\boldsymbol{x}^{(i-1)}\right)$$

if the inexact PG steps are sufficiently accurate and satisfy

$$\varepsilon^{(i)} \leq \sqrt{\delta^{(i)}}$$

where

$$\delta^{(i)} \triangleq \left\| \boldsymbol{x}^{(i)} - \boldsymbol{x}^{(i-1)} \right\|_2^2$$

is the local variation of signal iterates.

Convergence Criterion

$$\sqrt{\delta^{(i)}} < \epsilon \left\| \boldsymbol{x}^{(i)} \right\|_2$$

where $\epsilon > 0$ is the convergence threshold.

▸ more

Restart

The goal of *function* and *domain* restarts is to ensure that

- the PNPG iteration is *monotonic* and
- $\overline{\boldsymbol{x}}^{(i)}$ and $\boldsymbol{x}^{(i)}$ remain *within* $\operatorname{dom} f$.

▸ more

Summary of PNPG Approach

Combine

- convex-set projection with
- Nesterov acceleration.

Apply

- adaptive step size,
- restart.

more

Why?

- Thanks to step-size adaptation, no need for Lipschitz continuity of the gradient of the NLL.
- $\operatorname{dom} \mathcal{L}$ does not have to be $\mathbb{R}^p$.

Extends the application of the Nesterov's acceleration[†] to more general measurement models than those used previously.

[†] Y. Nesterov, "A method of solving a convex programming problem with convergence rate $O(1/k^2)$," *Sov. Math. Dokl.*, vol. 27, 1983, pp. 372–376.

Theorem (Convergence of the Objective Function)

Assume

- *NLL* $\mathcal{L}(\boldsymbol{x})$ *is convex and differentiable and* $\rho(\boldsymbol{x})$ *is convex,*
- $C \subseteq \operatorname{dom} \mathcal{L}$*: no need for domain restart.*

Consider the PNPG iteration without restart.

Theorem (Convergence of the Objective Function)

$$f\left(\boldsymbol{x}^{(k)}\right) - f\left(\boldsymbol{x}^{\star}\right) \leq \gamma^2 \frac{\left\|\boldsymbol{x}^{(0)} - \boldsymbol{x}^{\star}\right\|_2^2 + \mathcal{E}^{(k)}}{2\left(\sqrt{\beta^{(1)}} + \sum_{i=1}^{k} \sqrt{\beta^{(i)}}\right)^2}$$

where

$$\mathcal{E}^{(k)} \triangleq \sum_{i=1}^{k} \left(\theta^{(i)} \varepsilon^{(i)}\right)^2$$

error term, accounts for inexact PG steps

$$\boldsymbol{x}^{\star} \triangleq \arg\min_{\boldsymbol{x}} f(\boldsymbol{x}).$$

Comments

$$f\left(\boldsymbol{x}^{(k)}\right) - f\left(\boldsymbol{x}^{\star}\right) \leq \gamma^2 \frac{\left\|\boldsymbol{x}^{(0)} - \boldsymbol{x}^{\star}\right\|_2^2 + \mathcal{E}^{(k)}}{2\left(\sqrt{\beta^{(1)}} + \sum_{i=1}^{k} \sqrt{\beta^{(i)}}\right)^2}.$$

- Step sizes $\beta^{(i)}\uparrow$, convergence-rate upper bound $\downarrow$.
- better initialization, convergence-rate upper bound $\downarrow$.
- smaller prox-step approx. error, convergence-rate bound $\downarrow$.

Corollary

Under the condition of the Theorem,

$$f\left(\boldsymbol{x}^{(k)}\right) - f\left(\boldsymbol{x}^{\star}\right) \leq \underbrace{\gamma^2 \frac{\left\|\boldsymbol{x}^{(0)} - \boldsymbol{x}^{\star}\right\|_2^2 + \mathcal{E}^{(k)}}{2k^2 \beta_{\min}}}_{\mathcal{O}(k^{-2}) \text{ if } \mathcal{E}^{(+\infty)} < +\infty}$$

provided that

$$\beta_{\min} \triangleq \min_{k=1}^{+\infty} \beta^{(k)} > 0.$$

The assumption that the step-size sequence is lower-bounded by a strictly positive quantity is weaker than Lipschitz continuity of $\nabla \mathcal{L}(\boldsymbol{x})$ because it is guaranteed to have $\beta_{\min} > \xi / L$ if $\nabla \mathcal{L}(\boldsymbol{x})$ has a Lipschitz constant L.

Corollary

Under the condition of the Theorem,

$$f\left(\boldsymbol{x}^{(k)}\right) - f\left(\boldsymbol{x}^{\star}\right) \leq \underbrace{\gamma^2 \frac{\left\|\boldsymbol{x}^{(0)} - \boldsymbol{x}^{\star}\right\|_2^2 + \mathcal{E}^{(k)}}{2k^2 \beta_{\min}}}_{\mathcal{O}(k^{-2}) \text{ if } \mathcal{E}^{(+\infty)} < +\infty}$$

provided that

$$\beta_{\min} \triangleq \min_{k=1}^{+\infty} \beta^{(k)} > 0.$$

The assumption that the step-size sequence is lower-bounded by a strictly positive quantity is weaker than Lipschitz continuity of $\nabla \mathcal{L}(\boldsymbol{x})$ because it is guaranteed to have $\beta_{\min} > \xi / L$ if $\nabla \mathcal{L}(\boldsymbol{x})$ has a Lipschitz constant L.

Theorem (Convergence of Iterates)

Assume that

1. *NLL* $\mathcal{L}(\boldsymbol{x})$ *is convex and differentiable and* $r(\boldsymbol{x})$ *is convex,*
2. $C \subseteq \operatorname{dom} \mathcal{L}$, *hence no need for domain restart,*
3. *cumulative error term* $\mathcal{E}^{(k)}$ *converges:* $\mathcal{E}^{(+\infty)} < +\infty$,
4. *momentum tuning constants satisfy* $\gamma > 2$ *and* $b \in \left[0, 1/\gamma^2\right]$,
5. *the step-size sequence* $\left(\beta^{(i)}\right)_{i=1}^{+\infty}$ *is bounded within the range* $\left[\beta_{\min}, \beta_{\max}\right]$, $(\beta_{\min} > 0)$.

☞ The *sequence of PNPG iterates* $\boldsymbol{x}^{(i)}$ *without restart converges weakly to a minimizer of* $f(\boldsymbol{x})$. *a minimizer of* $f(\boldsymbol{x})$.

Theorem (Convergence of Iterates)

strict inequality

Assume that

1. *NLL* $\mathcal{L}(\boldsymbol{x})$ *is convex and differentiable and* $r(\boldsymbol{x})$ *is convex,*
2. $C \subseteq \operatorname{dom} \mathcal{L}$, *hence no need for domain restart,*
3. *cumulative error term* $\mathcal{E}^{(k)}$ *converges:* $\mathcal{E}^{(+\infty)} < +\infty$,
4. *momentum tuning const. satisfy* $\gamma > 2$ *and* $b \in \left[0, 1/\gamma^2\right]$,
5. *the step-size sequence* $\left(\beta^{(i)}\right)_{i=1}^{+\infty}$ *is bounded within the range* $\left[\beta_{\min}, \beta_{\max}\right]$, $(\beta_{\min} > 0)$.

☞ The *sequence of PNPG iterates* $\boldsymbol{x}^{(i)}$ *without restart converges weakly to a minimizer of* $f(\boldsymbol{x})$. *a minimizer of* $f(\boldsymbol{x})$.

narrower than $\left[0, 1/4\right]$

Idea of Proof.

Recall the inequality

$$\theta^{(i)} = \tfrac{1}{\gamma} + \sqrt{b + B^{(i)}\left(\theta^{(i-1)}\right)^2} \leq \tfrac{1}{2} + \sqrt{\tfrac{1}{4} + B^{(i)}\left(\theta^{(i-1)}\right)^2}$$

used to establish convergence of the objective function.
Assumption 4:

$$\gamma > 2, \qquad b \in \left[0, 1/\gamma^2\right]$$

creates a sufficient "gap" in this inequality that allows us to

- show faster convergence of the objective function than the previous theorem and
- establish the convergence of iterates.

☞ Inspired by (Chambolle and Dossal 2015).

□

Introduction

Signal reconstruction from Poisson-distributed measurements with affine model for the mean-signal intensity is important for

- tomographic (Ollinger and Fessler 1997),
- astronomic, optical, microscopic (Bertero *et al.* 2009),
- hyperspectral (Willett *et al.* 2014)

imaging.

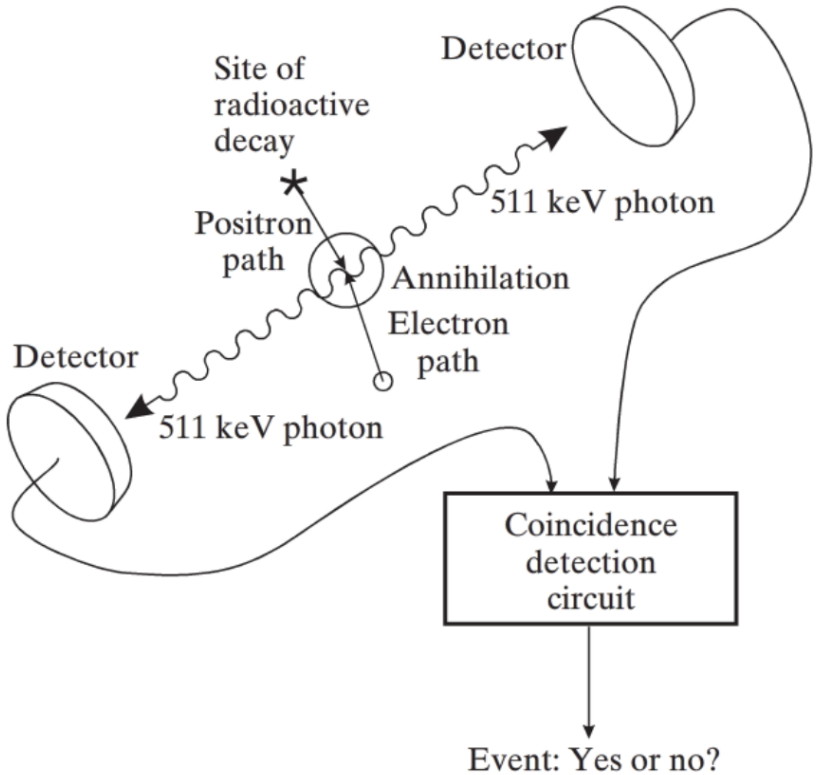

PET: Coincidence detection due to positron decay and annihilation (Prince and Links 2015).

Measurement Model

N independent measurements $\boldsymbol{y} = (y_n)_{n=1}^N$ follow the Poisson distribution with means

$$[\Phi \boldsymbol{x} + \boldsymbol{b}]_n$$

where

$$\Phi \in \mathbb{R}_+^{N \times p}, \qquad \boldsymbol{b}$$

are the *known* sensing matrix and intercept term[‡].

[‡] the intercept $\boldsymbol{b}$ models background radiation and scattering, obtained, e.g., by calibration before the measurements $\boldsymbol{y}$ have been collected

Existing Work

The sparse Poisson-intensity reconstruction algorithm (SPIRAL)[§]

- approximates the logarithm function in the underlying NLL by adding a small positive term to it and then
- descends a regularized NLL objective function with proximal steps that employ Barzilai-Borwein (BB) step size in each iteration, followed by backtracking.

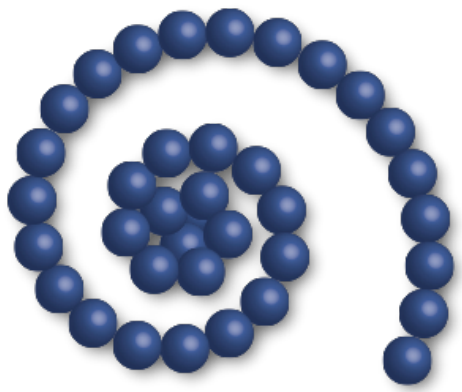

[§]Z. T. Harmany *et al.*, "This is SPIRAL-TAP: Sparse Poisson intensity reconstruction algorithms—theory and practice," *IEEE Trans. Image Process.*, vol. 21, no. 3, pp. 1084–1096, Mar. 2012.

PET Image Reconstruction

- 128×128 concentration map $\boldsymbol{x}$.
- Collect the photons from 90 equally spaced directions over $180°$, with 128 radial samples at each direction,
- Background radiation, scattering effect, and accidental coincidence combined together lead to a known intercept term $\boldsymbol{b}$.
- The elements of the intercept term are set to a constant equal to 10 % of the sample mean of $\Phi\boldsymbol{x}$: $\boldsymbol{b} = \dfrac{\mathbf{1}^T \Phi \boldsymbol{x}}{10N}\mathbf{1}$.

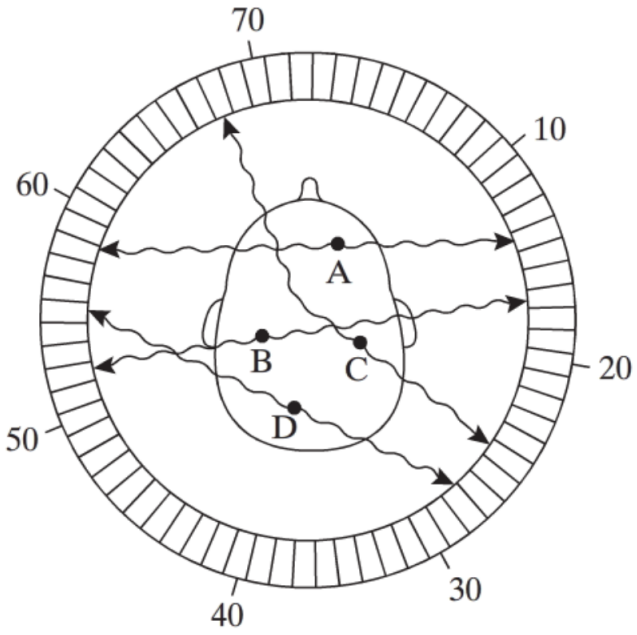

The model, choices of parameters in the PET system setup, and concentration map have been adopted from Image Reconstruction Toolbox (IRT) (Fessler 2016).

Compared Methods

- Filtered backprojection (FBP) (Ollinger and Fessler 1997) and
- PG methods that aim at minimizing $f(\boldsymbol{x})$ with nonnegative $\boldsymbol{x}$:

$$\boldsymbol{C} = \mathbb{R}^{\boldsymbol{p}}_{+}.$$

All iterative methods initialized by FBP reconstructions.

Matlab implementation available at
`http://isucsp.github.io/imgRecSrc/npg.html`.

PG Methods

- PNPG with $(\gamma, b) = (2, 1/4)$.
- AT (Auslender and Teboulle 2006) implemented in the templates for first-order conic solvers (TFOCS) package (Becker *et al.* 2011) with a periodic restart every 200 iterations (tuned for its best performance) and our proximal mapping.
- SPIRAL, when possible.

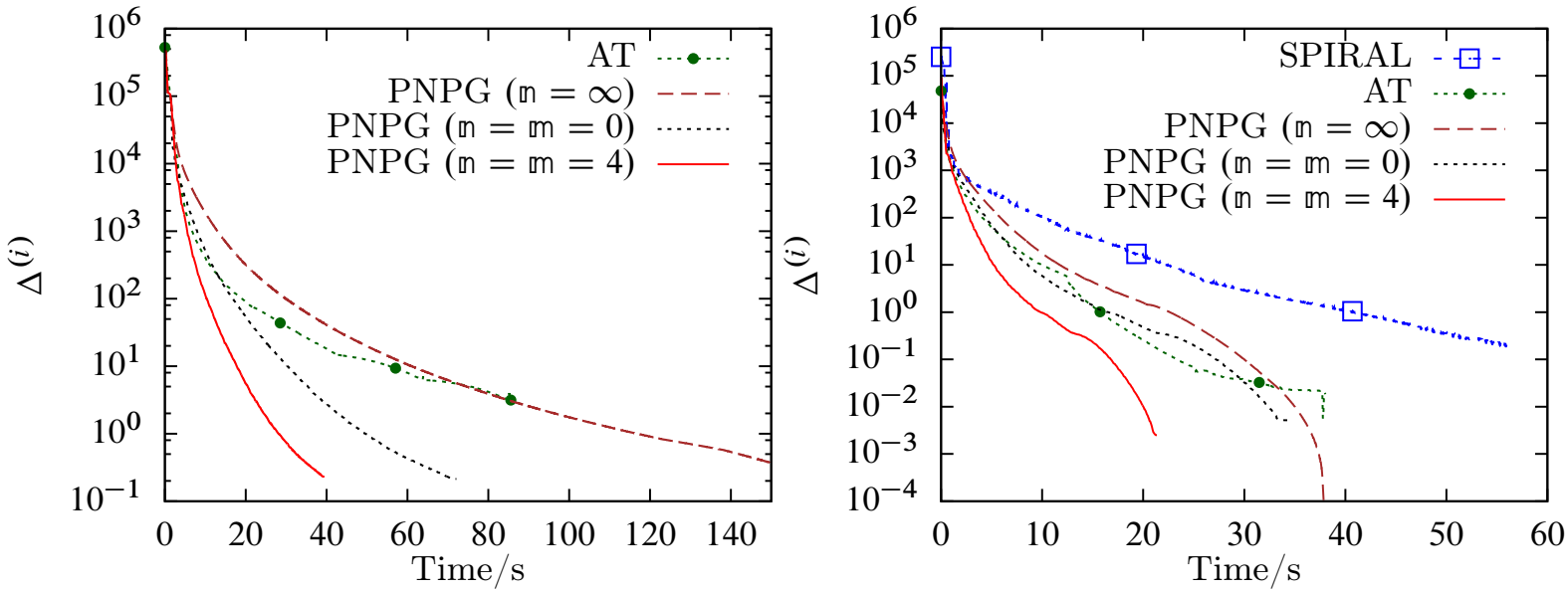

(a) DWT, $\mathbf{1}^T \mathrm{E}(\boldsymbol{y}) = 10^8$ (b) TV, $\mathbf{1}^T \mathrm{E}(\boldsymbol{y}) = 10^7$

Figure 3: Centered objectives as functions of CPU time.

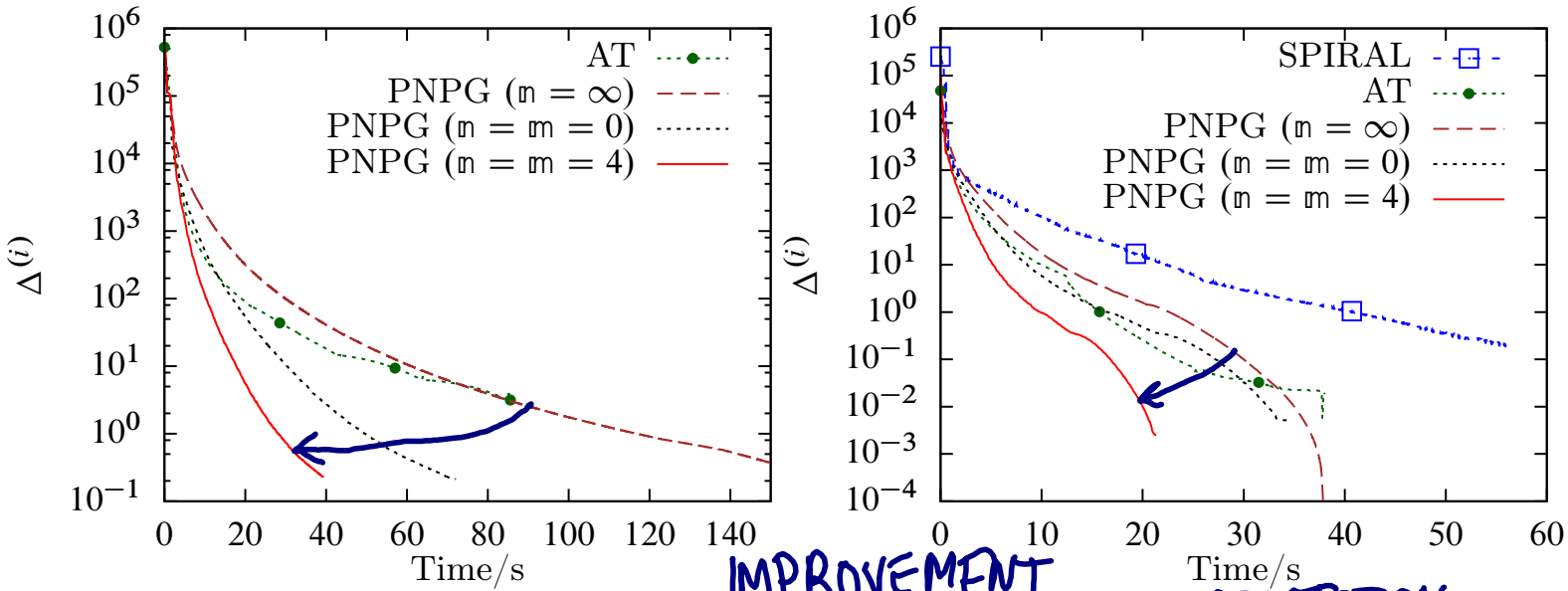

(a) ℓ_1, $\mathbf{1}^T \mathrm{E}(\boldsymbol{y}) = 10^8$ (b) TV, $\mathbf{1}^T \mathrm{E}(\boldsymbol{y}) = 10^7$

Figure 7: Centered objectives as functions of CPU time.

Linear Model with Gaussian Noise

$$\mathcal{L}(\boldsymbol{x}) = \frac{1}{2}\|\boldsymbol{y} - \Phi\boldsymbol{x}\|_2^2$$

where

- $\boldsymbol{y} \in \mathbb{R}^N$ is the measurement vector and
- the elements of the sensing matrix Φ are independent, identically distributed (i.i.d.), drawn from the standard normal distribution.

We select the DWT sparsifying signal transform.

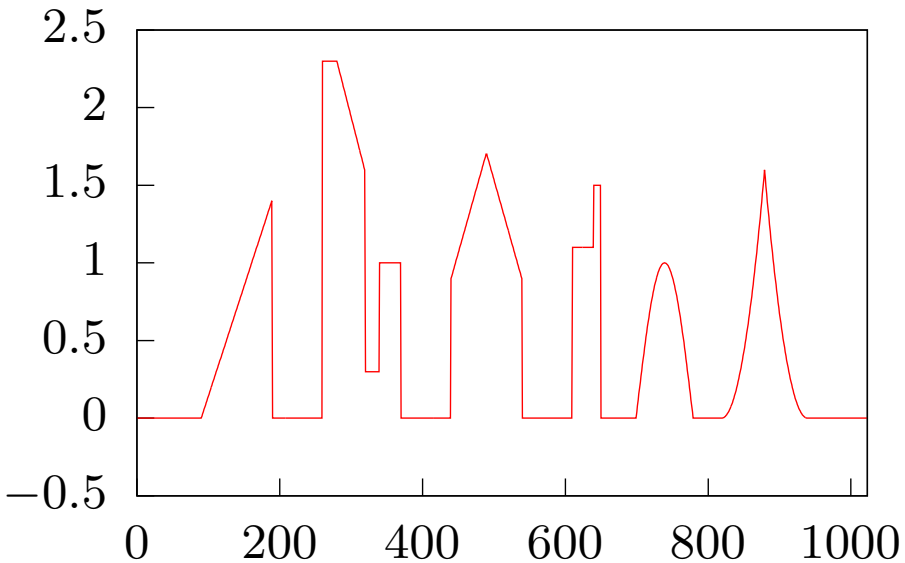

Figure 4: True signal.

Comments

- More methods available for comparison:
  - sparse reconstruction by separable approximation (SpaRSA) (Wright *et al.* 2009),
  - generalized forward-backward (GFB) (Raguet *et al.* 2013),
  - primal-dual splitting (PDS) (Condat 2013).
- Select the regularization parameter u as

$$u = 10^a U, \qquad U \triangleq \left\| \Psi^T \nabla \mathcal{L}(\mathbf{0}) \right\|_\infty$$

  where a is an integer selected from the interval $[-9, -1]$ and U is an upper bound on u of interest.
- Choose the nonnegativity convex set:

$$C = \mathbb{R}^p_+.$$

- If we remove the convex-set constraint by setting $C = \mathbb{R}^p$, PNPG iteration reduces to the Nesterov's proximal gradient iteration with adaptive step size that imposes signal sparsity *only* in the analysis form (termed NPG$_\mathsf{S}$).

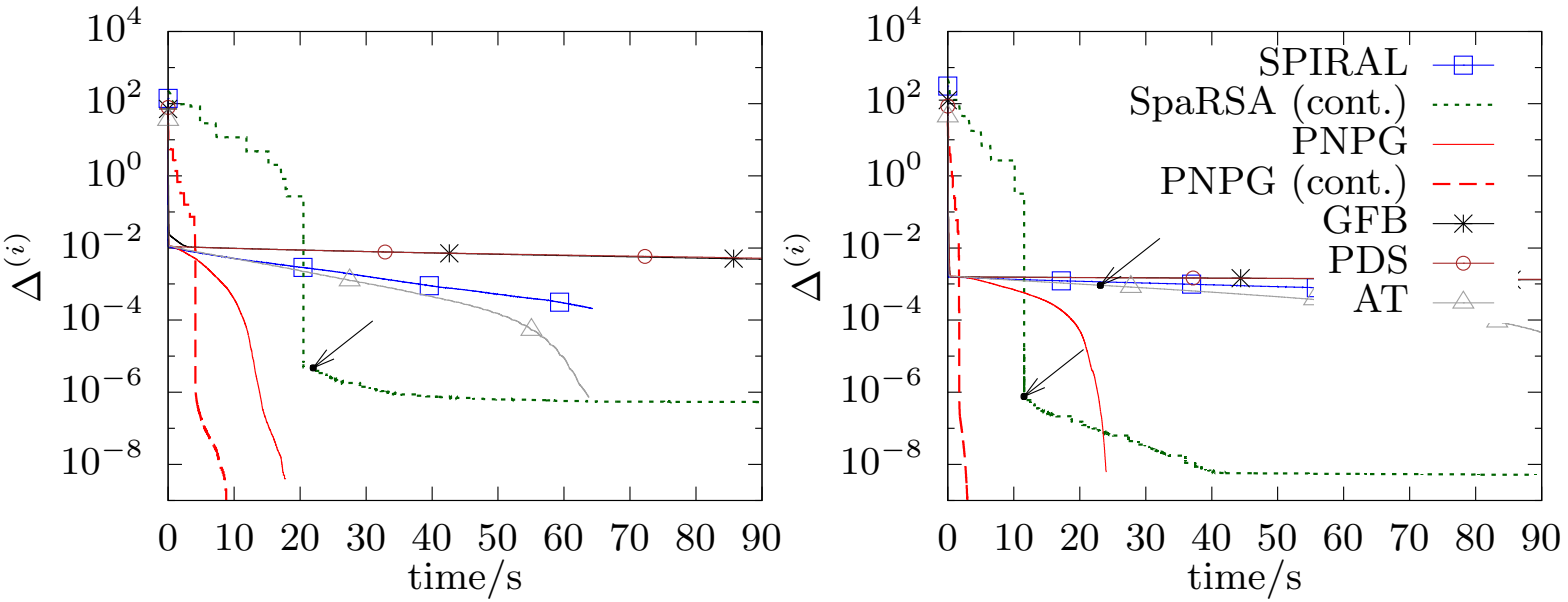

(a) $a = -5, N/p = 0.34$ (b) $a = -6, N/p = 0.49$

Figure 5: Centered objectives as functions of CPU time.

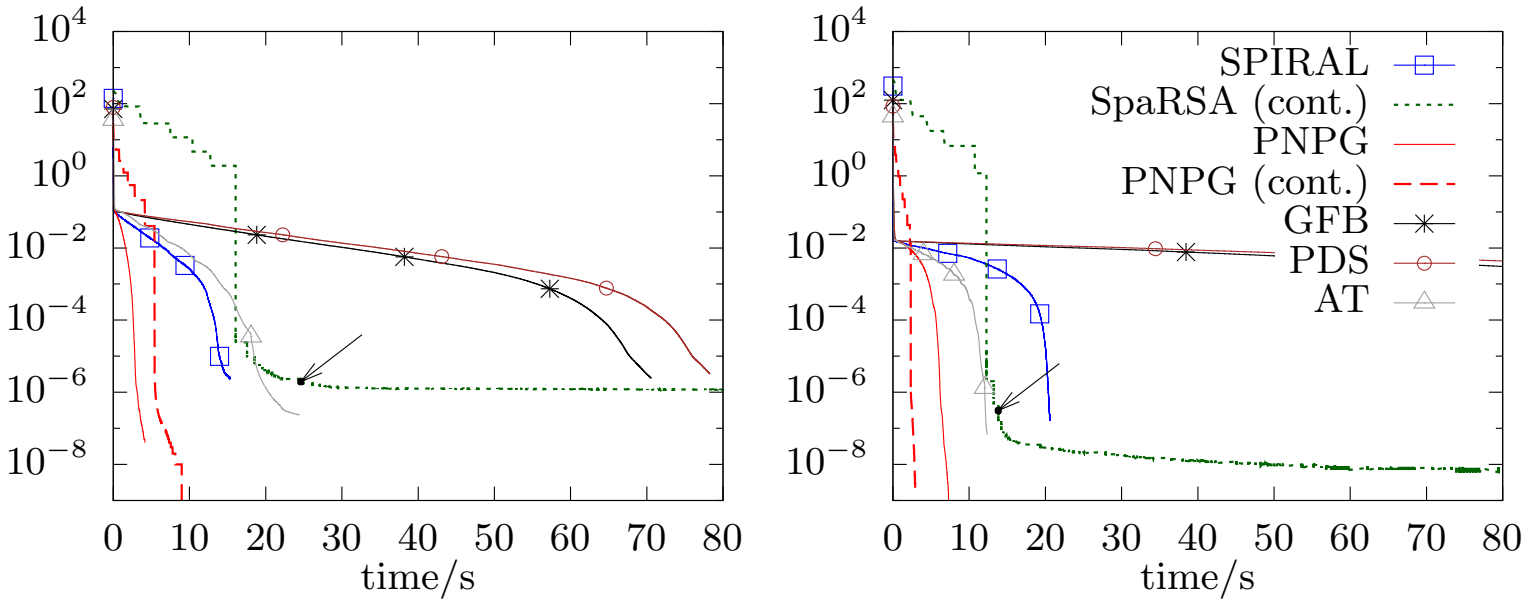

(a) $a = -4, N/p = 0.34$ (b) $a = -5, N/p = 0.49$

Figure 6: Centered objectives as functions of CPU time.

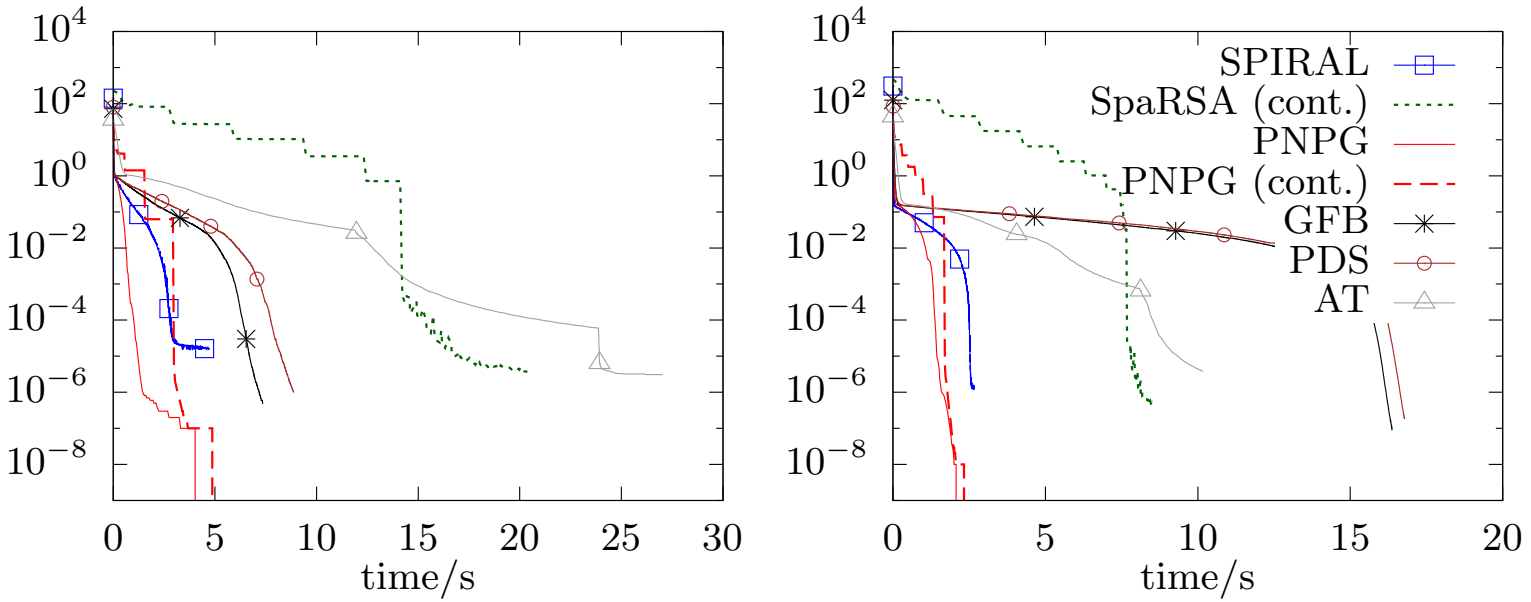

(a) $a = -3, N/p = 0.34$ (b) $a = -4, N/p = 0.49$

Figure 7: Centered objectives as functions of CPU time.

Publications

- R. G. and A. D. (Oct. 2016), Projected Nesterov's proximal-gradient algorithm for sparse signal reconstruction with a convex constraint, version 6. arXiv: 1502.02613 [stat.CO].
- R. G. and A. D., "Projected Nesterov's proximal-gradient signal recovery from compressive Poisson measurements," *Proc. Asilomar Conf. Signals, Syst. Comput.*, Pacific Grove, CA, Nov. 2015, pp. 1490–1495. doi: 10.1109/ACSSC.2015.7421393.

More Terminology and Notation

- $\iota^{\mathsf{L}}(s)$ is the *Laplace transform* of $\iota(\kappa)$:

$$\iota^{\mathsf{L}}(s) \triangleq \int \iota(\kappa) \mathrm{e}^{-s\kappa} \, \mathrm{d}\kappa,$$

- Laplace transform with vector argument:

$$\boldsymbol{b}_{\circ}^{\mathsf{L}}(\boldsymbol{s}) = \boldsymbol{b}_{\circ}^{\mathsf{L}}\left(\begin{bmatrix} s_1 \\ s_2 \\ \vdots \\ s_N \end{bmatrix}\right) = \begin{bmatrix} \boldsymbol{b}^{\mathsf{L}}(s_1) \\ \boldsymbol{b}^{\mathsf{L}}(s_2) \\ \vdots \\ \boldsymbol{b}^{\mathsf{L}}(s_N) \end{bmatrix}.$$

X-ray CT

An X-ray CT scan consists of multiple projections with the beam intensity measured by multiple detectors.

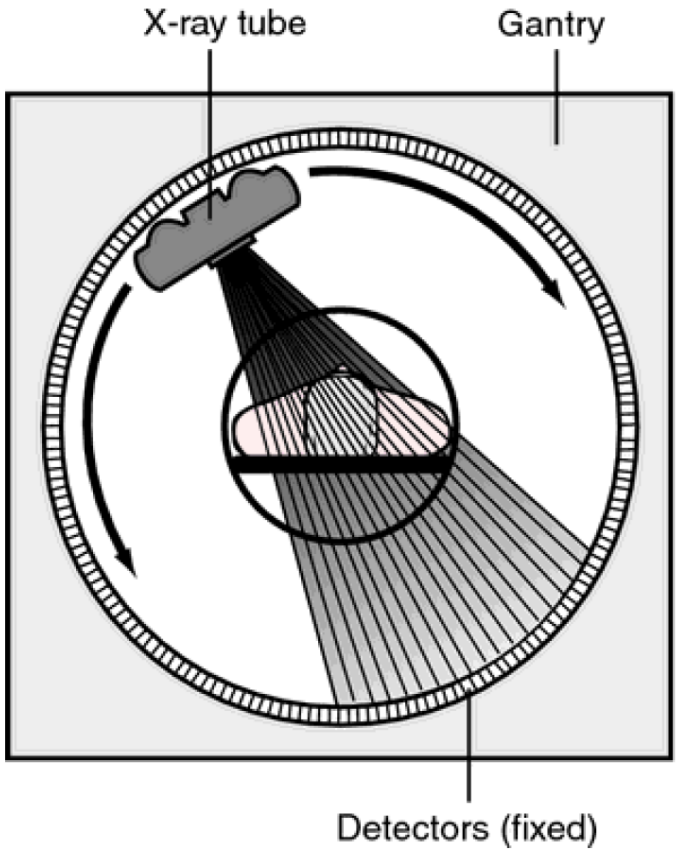

Figure 8: Fan-beam CT system.

Exponential Law of Absorption

The fraction $\mathrm{d}\mathcal{I}/\mathcal{I}$ of plane-wave intensity lost in traversing an infinitesimal thickness $\mathrm{d}\ell$ at Cartesian coordinates (x, y) is proportional to $\mathrm{d}\ell$:

$$\frac{\mathrm{d}\mathcal{I}}{\mathcal{I}} = -\underbrace{\mu(x, y, \varepsilon)}_{\text{attenuation}}\,\mathrm{d}\ell = -\underbrace{\kappa(\varepsilon)\alpha(x, y)}_{\text{separable}}\,\mathrm{d}\ell$$

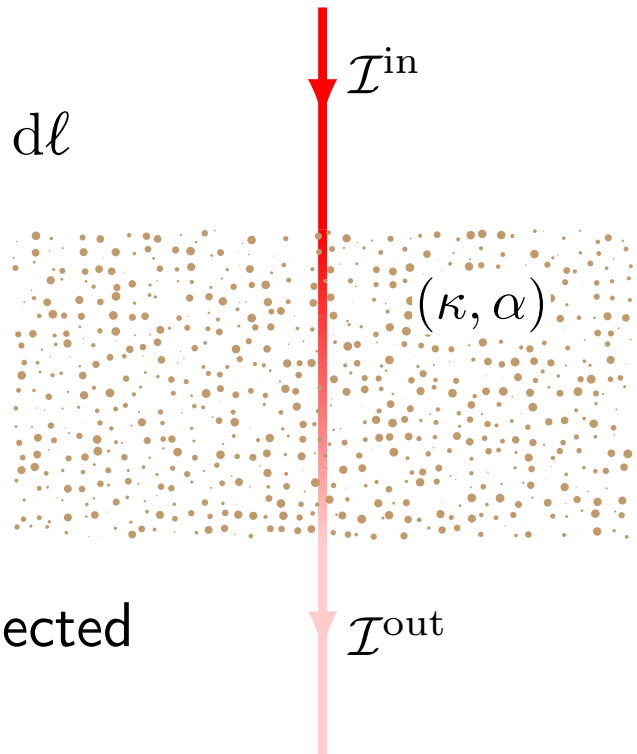

where

- $\kappa(\varepsilon) \geq 0$ is the mass attenuation function of the material,
- $\alpha(x, y) \geq 0$ is the density map of the inspected object, and
- ε is photon energy.

To obtain the intensity decrease along a straight-line path $\ell = \ell(x, y)$, integrate along ℓ and over ε. The underlying measurement model is nonlinear.

Polychromatic X-ray CT Model

- Incident energy $\mathcal{I}^{\text{in}}$ spreads along photon energy ε with density $\iota(\varepsilon)$:

$$\int \iota(\varepsilon)\,\mathrm{d}\varepsilon = \mathcal{I}^{\text{in}}.$$

- Noiseless energy measurement obtained upon traversing a straight line $\ell = \ell(x, y)$ through an object composed of a single material:

$$\mathcal{I}^{\text{out}} = \int \iota(\varepsilon) \exp\left[-\kappa(\varepsilon) \int_{\ell} \alpha(x, y)\,\mathrm{d}\ell\right] \mathrm{d}\varepsilon.$$

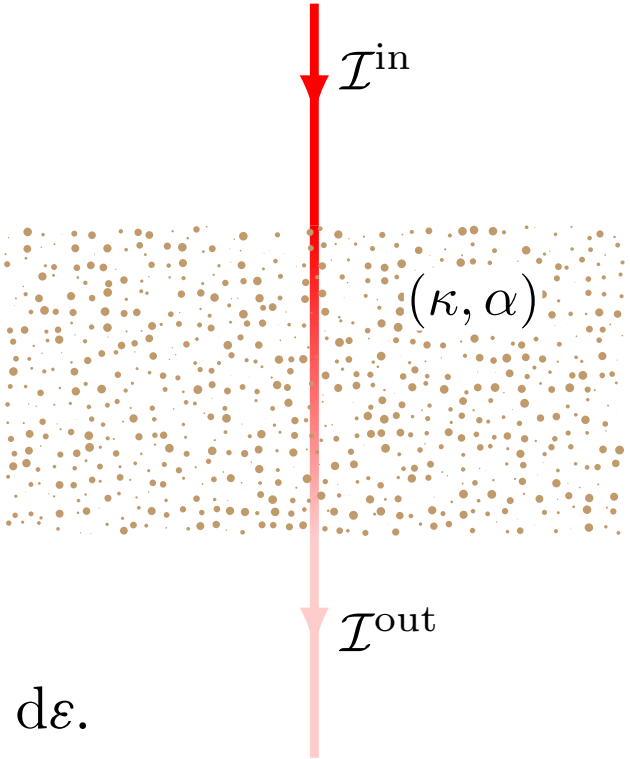

Linear Reconstruction Artifacts

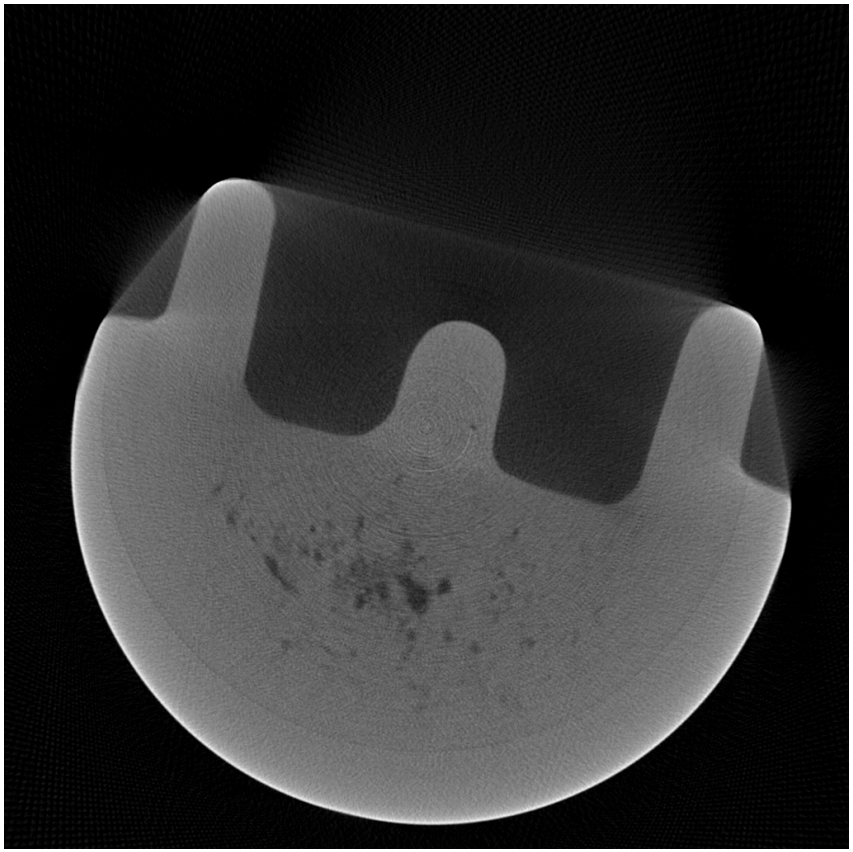

Figure 9: FBP reconstruction of an industrial object.

Note the cupping and streaking artifacts of the linear FBP reconstruction, applied to $\ln \mathcal{I}^{\text{out}}$.

Problem Formulation and Goal

Assume that both

- the incident spectrum $\iota(\varepsilon)$ of X-ray source and
- mass attenuation function $\kappa(\varepsilon)$ of the object

are unknown.

Goal: Estimate the density map $\alpha(x, y)$.

Problem Formulation and Goal

Assume that both

- the incident spectrum $\iota(\varepsilon)$ of X-ray source and
- mass attenuation function $\kappa(\varepsilon)$ of the object

are unknown.

Goal: Estimate the density map $\alpha(x, y)$.

Polychromatic X-ray CT Model Using Mass-Attenuation Spectrum

- Mass attenuation $\kappa(\varepsilon)$ and incident spectrum density $\iota(\varepsilon)$ are both functions of ε.
- **Idea.** Write the model as integrals of κ rather than ε:

$$\mathcal{I}^{\text{in}} = \int \iota(\kappa)\,\mathrm{d}\kappa = \iota^{\mathsf{L}}(0)$$

$$\mathcal{I}^{\text{out}} = \int \iota(\kappa) \exp\left[-\kappa \int_{\ell} \alpha(x,y)\,\mathrm{d}\ell\right] \mathrm{d}\kappa = \iota^{\mathsf{L}}\left(\int_{\ell} \alpha(x,y)\,\mathrm{d}\ell\right)$$

.

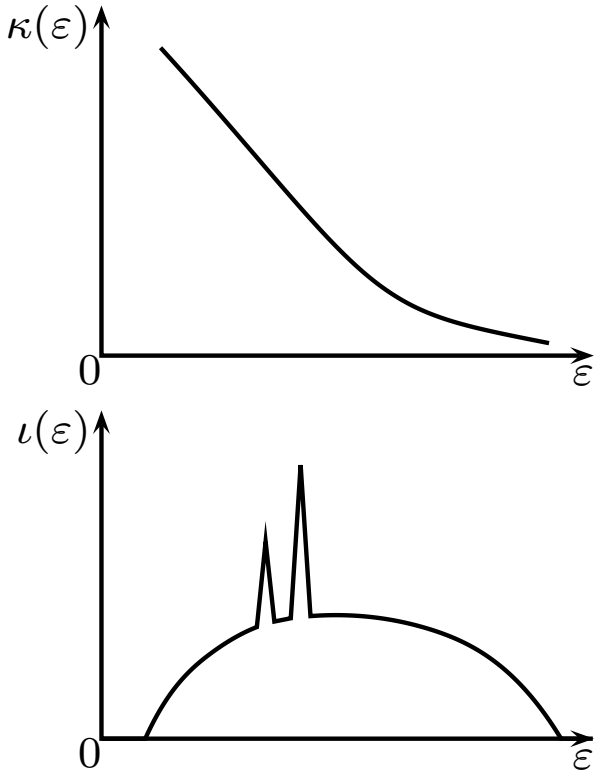

☞ Need to estimate one function, $\iota(\kappa)$, rather than two, $\iota(\varepsilon)$ and $\kappa(\varepsilon)$!

Polychromatic X-ray CT Model Using Mass-Attenuation Spectrum

- Mass attenuation $\kappa(\varepsilon)$ and incident spectrum density $\iota(\varepsilon)$ are both functions of ε.
- **Idea.** Write the model as integrals of κ rather than ε:

$$\mathcal{I}^{\text{in}} = \int \iota(\kappa)\,\mathrm{d}\kappa = \iota^{\mathsf{L}}(0)$$

$$\mathcal{I}^{\text{out}} = \int \iota(\kappa)\exp\left[-\kappa\int_{\ell}\alpha(x,y)\,\mathrm{d}\ell\right]\mathrm{d}\kappa = \iota^{\mathsf{L}}\left(\int_{\ell}\alpha(x,y)\,\mathrm{d}\ell\right)$$

.

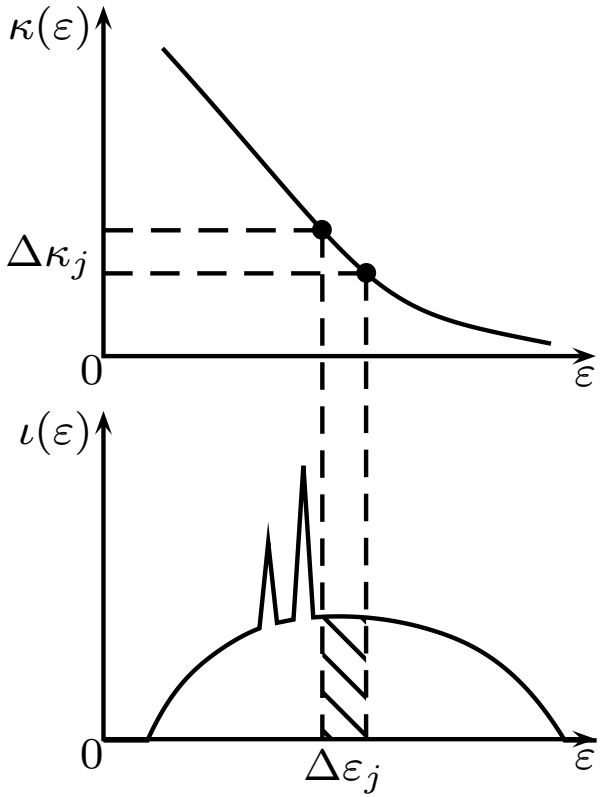

☞ Need to estimate one function, $\iota(\kappa)$, rather than two, $\iota(\varepsilon)$ and $\kappa(\varepsilon)$!

Mass-Attenuation Spectrum

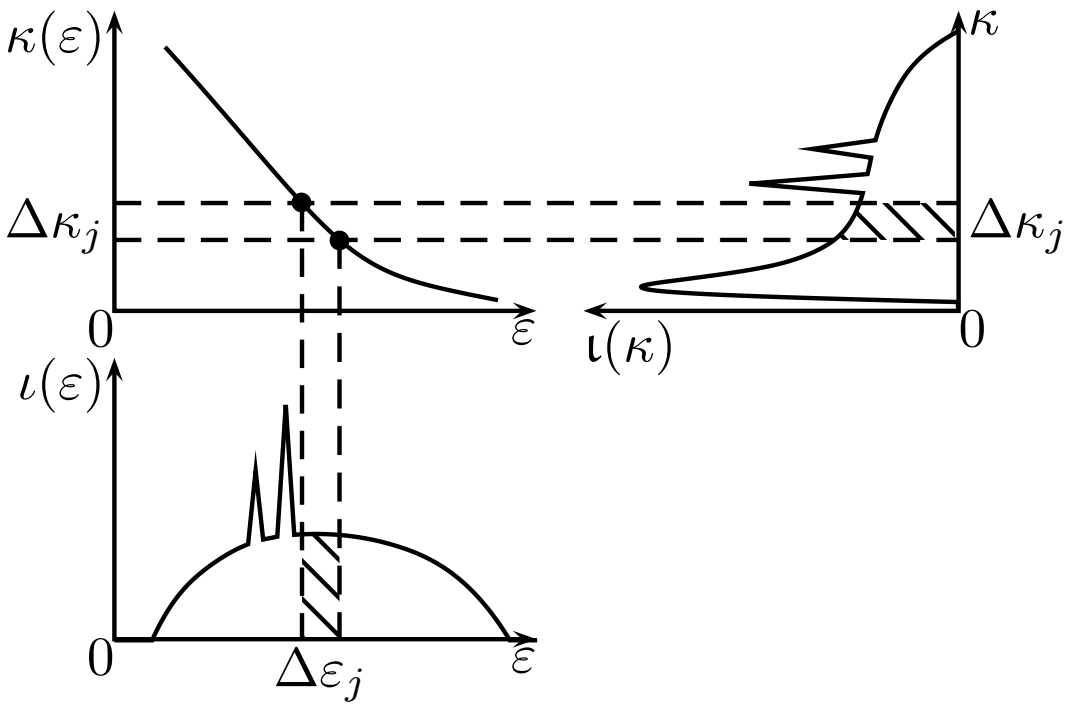

Figure 10: Relationship between mass attenuation κ, incident spectrum ι, photon energy ε, and mass attenuation spectrum $\iota(\kappa)$.

Basis-function expansion of mass-attenuation spectrum $\iota(\kappa) = \boldsymbol{b}(\kappa)\mathcal{I}$

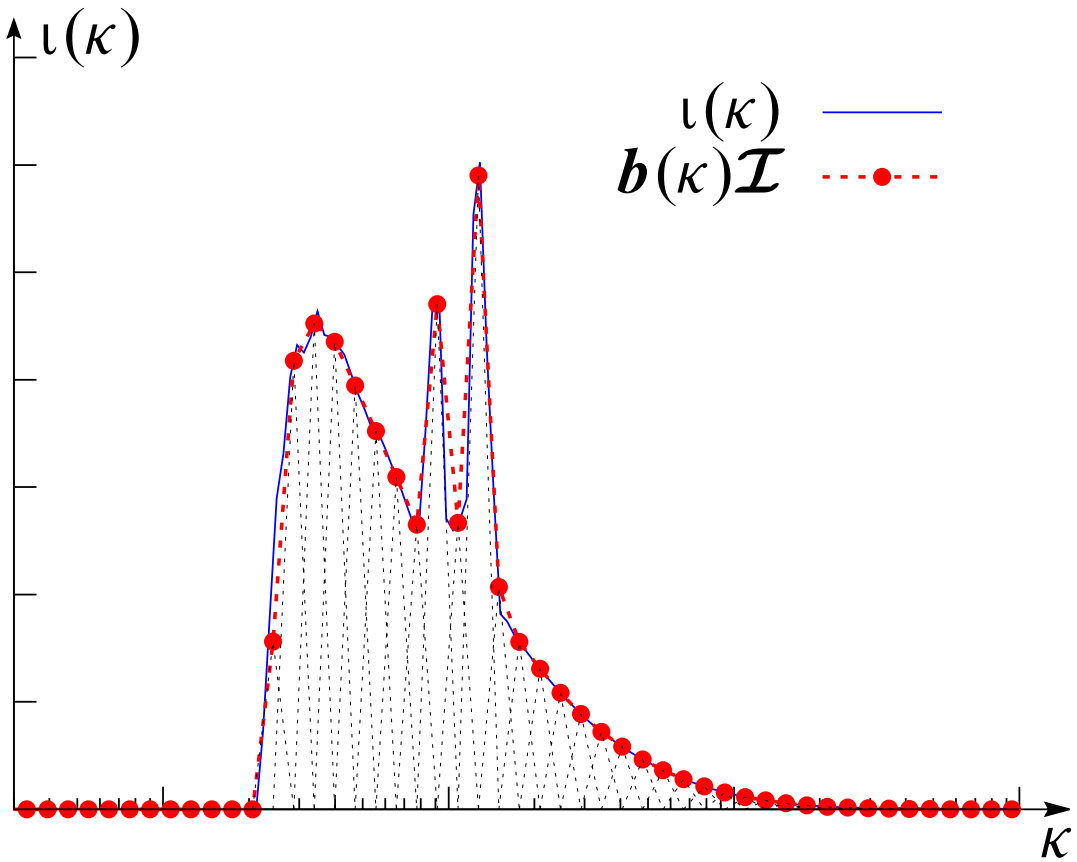

Figure 11: B1-spline expansion $\iota(\kappa) = \boldsymbol{b}(\kappa)\mathcal{I}$, where the B1-spline basis is $\underbrace{\boldsymbol{b}(\kappa)}_{1\times J} = \big[b_1(\kappa), b_2(\kappa), \ldots, b_J(\kappa)\big]$. $\iota(\kappa) \geq 0$ implies $\mathcal{I} \succeq \mathbf{0}$.

Noiseless Measurement Model

$N \times 1$ vector of noiseless energy measurements:

$$\mathcal{I}^{\text{out}}(\boldsymbol{x}, \mathcal{I}) = \boldsymbol{b}_{\circ}^{\mathsf{L}}(\Phi \boldsymbol{x})\mathcal{I}$$

where Φ is the known projection matrix,

- $\boldsymbol{x} = \left(\boldsymbol{x}_i\right)_{i=1}^{p} \succeq \mathbf{0}$ is an *unknown* $p \times 1$ density-map vector representing the 2D image we wish to reconstruct, and
- $$\mathcal{I} = \left(\mathcal{I}_j\right)_{j=1}^{J} \succeq \mathbf{0}$$

  is an *unknown* $J \times 1$ vector of corresponding mass-attenuation basis-function coefficients.

Poisson Noise Model

For independent Poisson measurements $\boldsymbol{\mathcal{E}} = (\mathcal{E}_n)_{n=1}^N$, the NLL is

$$\mathcal{L}(\boldsymbol{x}, \boldsymbol{\mathcal{I}}) = \mathbf{1}^T \left[\boldsymbol{\mathcal{I}}^{\text{out}}(\boldsymbol{x}, \boldsymbol{\mathcal{I}}) - \boldsymbol{\mathcal{E}}\right] - \sum_{n, \mathcal{E}_n \neq 0} \mathcal{E}_n \ln \frac{\mathcal{I}_n^{\text{out}}(\boldsymbol{x}, \boldsymbol{\mathcal{I}})}{\mathcal{E}_n}.$$

Penalized NLL

- objective function

$$f(\boldsymbol{x},\mathcal{I}) = \mathcal{L}(\boldsymbol{x},\mathcal{I}) + u \underbrace{\left[\|\Psi^T \boldsymbol{x}\|_1 + \mathbb{I}_C(\boldsymbol{x})\right]}_{r(\boldsymbol{x})} + \mathbb{I}_{\mathbb{R}^J_+}(\mathcal{I})$$

- NLL
- penalty term
  $u > 0$ is a scalar tuning constant
  we select gradient map sparsifying transform,
  $C = \mathbb{R}^J_+$

Penalized NLL

- objective function

$$f(\boldsymbol{x},\mathcal{I}) = \mathcal{L}(\boldsymbol{x},\mathcal{I}) + u \underbrace{\left[\|\Psi^T \boldsymbol{x}\|_1 + \mathbb{I}_C(\boldsymbol{x})\right]}_{r(\boldsymbol{x})} + \mathbb{I}_{\mathbb{R}_+^J}(\mathcal{I})$$

- NLL
- penalty term

  $u > 0$ is a scalar tuning constant

  we select gradient map sparsifying transform, $C = \mathbb{R}_+^J$

Penalized NLL

- objective function

$$f(\boldsymbol{x},\mathcal{I}) = \mathcal{L}(\boldsymbol{x},\mathcal{I}) + u \underbrace{\left[\|\Psi^T \boldsymbol{x}\|_1 + \mathbb{I}_C(\boldsymbol{x})\right]}_{r(\boldsymbol{x})} + \mathbb{I}_{\mathbb{R}_+^J}(\mathcal{I})$$

- NLL
- penalty term

$u > 0$ is a scalar tuning constant

we select gradient map sparsifying transform, $C = \mathbb{R}_+^J$

Goal and Minimization Approach

Goal: Estimate the density-map and mass-attenuation spectrum parameters

$$(\boldsymbol{x}, \mathcal{I})$$

by minimizing the penalized NLL $f(\boldsymbol{x}, \mathcal{I})$.
Approach: A block coordinate-descent that uses

- Nesterov's proximal-gradient (NPG) (Nesterov 1983) and
- limited-memory Broyden-Fletcher-Goldfarb-Shanno with box constraints (L-BFGS-B) (Byrd *et al.* 1995; Zhu *et al.* 1997)

methods to update estimates of the density map and mass-attenuation spectrum parameters.
We refer to this iteration as NPG-BFGS algorithm.

Numerical Examples

- convergence threshold:

$$\epsilon = 10^{-6}$$

- B1-spline constants set to satisfy

$$\begin{aligned} J &= 20, && \text{\# basis functions} \\ q^J &= 10^3, && \text{span} \\ \kappa_0 q^{\lceil 0.5(J+1) \rceil} &= 1, && \text{centering} \end{aligned}$$

Implementation available at github.com/isucsp/imgRecSrc.

Simulated X-ray CT Example

- Equi-spaced fan-beam projections over $360°$,
- X-ray source to rotation center is $2000\times$ detector size,
- measurement array size of 512 elements, and
- image to reconstruct has size 512×512.

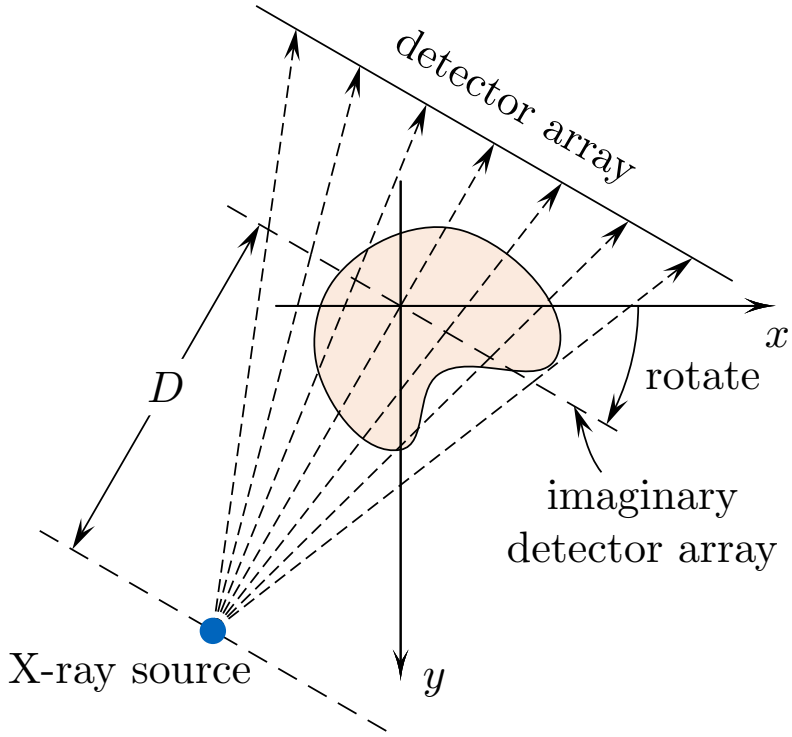

- performance metric is the relative square error (RSE) of an estimate $\hat{\boldsymbol{x}}$ of the signal coefficient vector:

$$\mathrm{RSE}\{\hat{\boldsymbol{x}}\} = 1 - \left(\frac{\hat{\boldsymbol{x}}^T \boldsymbol{x}_{\mathsf{true}}}{\|\hat{\boldsymbol{x}}\|_2 \|\boldsymbol{x}_{\mathsf{true}}\|_2} \right)^2 .$$

Simulated X-ray CT Example

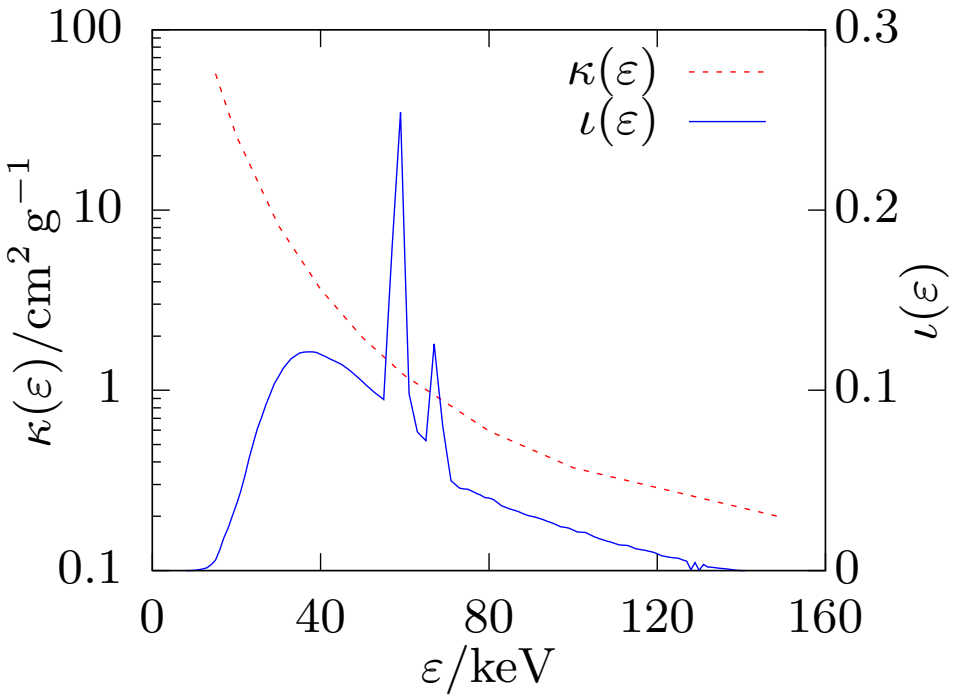

- Incident X-ray spectrum from tungsten anode X-ray tubes at 140 keV with 5 % relative voltage ripple, and
- using photon-energy discretization with 130 equi-spaced discretization points over the range 20 keV to 140 keV.

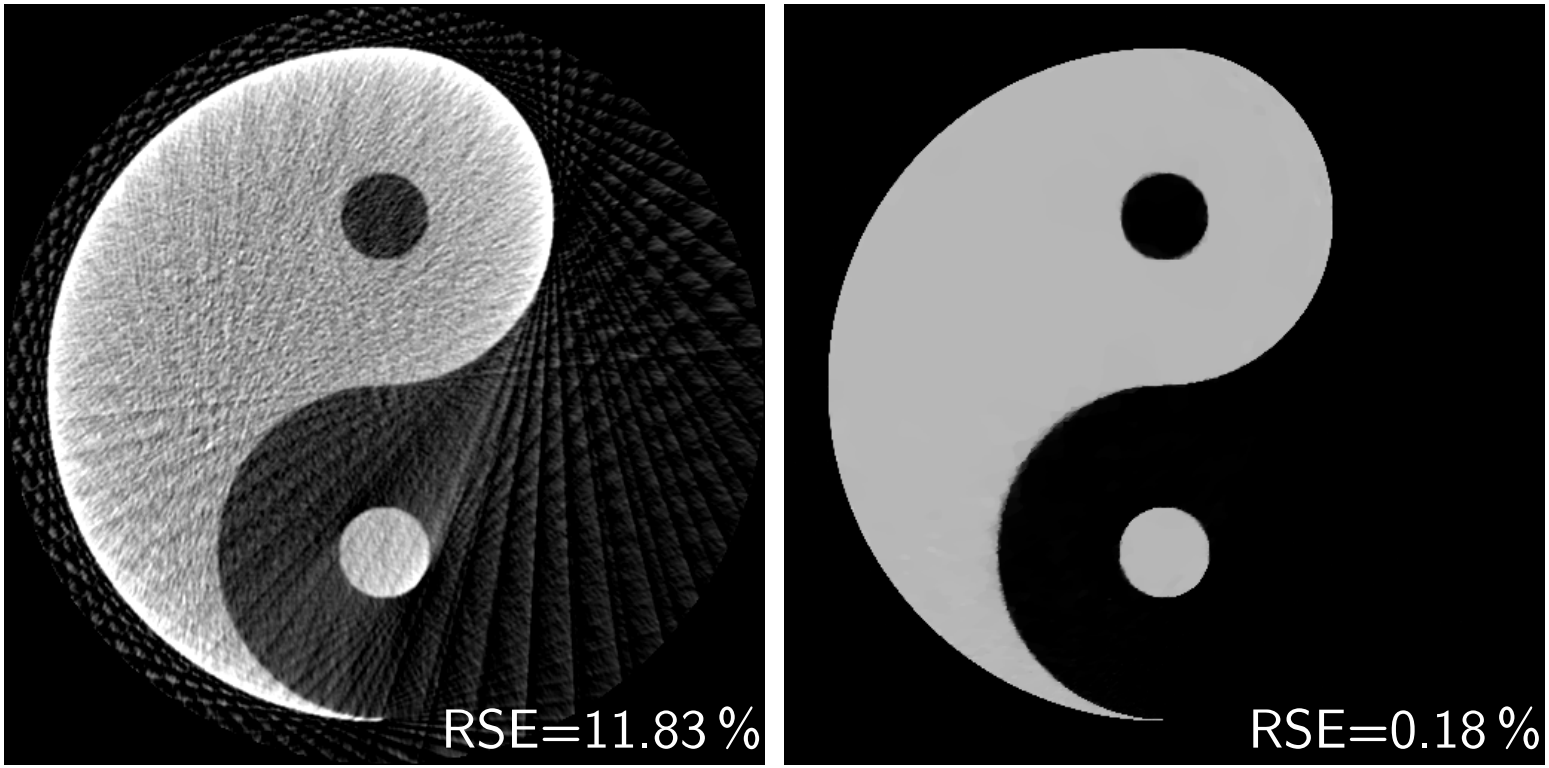

(a) FBP (b) NPG-BFGS

Figure 12: Reconstructions from 60 projections.

Simulated X-ray CT Example

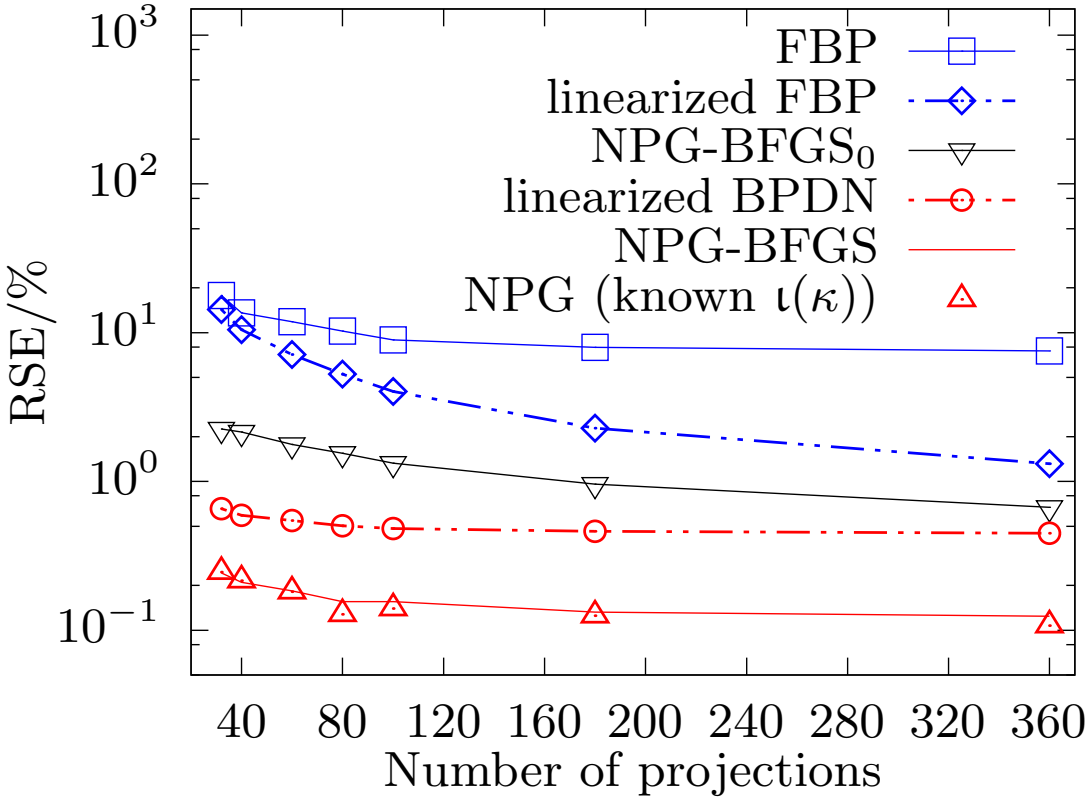

Figure 13: Average RSEs as functions of the number of projections.

Real X-ray CT Example I

- 360 equi-spaced fan-beam projections with 1° spacing,
- X-ray source to rotation center is $3492\times$ detector size,
- measurement array size of 694 elements,
- projection matrix Φ constructed directly on GPU (multi-thread version on CPU is also available) with full circular mask (D. *et al.* 2011),

yielding a nonlinear estimation problem with $N = 694 \times 360$ measurements and an 512×512 image to reconstruct.

Real data provided by Joe Gray, CNDE. Thanks!

Real X-ray CT Example I

- 360 equi-spaced fan-beam projections with 1° spacing,
- X-ray source to rotation center is $3492\times$ detector size,
- measurement array size of 694 elements,
- projection matrix Φ constructed directly on GPU (multi-thread version on CPU is also available) with full circular mask (D. *et al.* 2011).

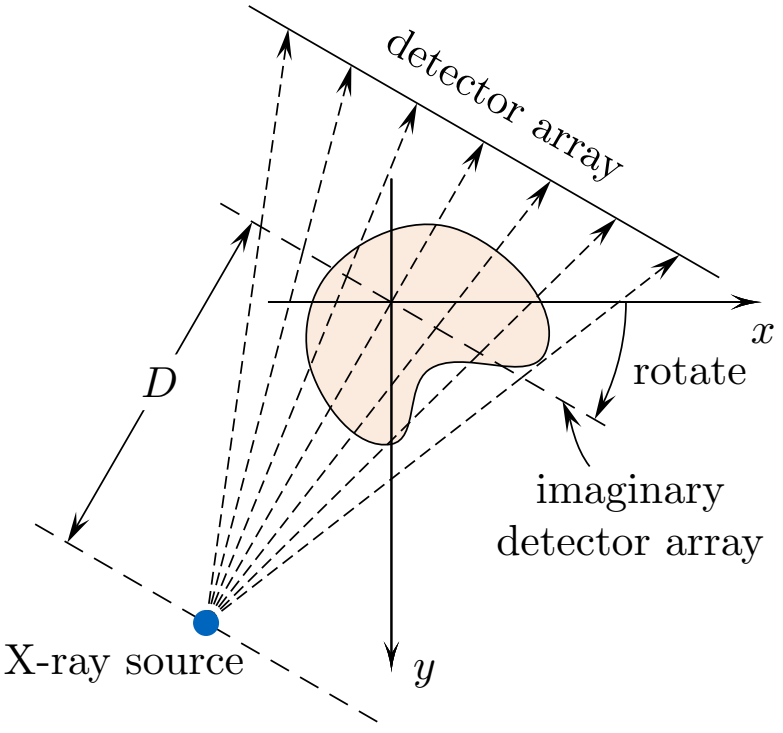

yielding a nonlinear estimation problem with $N = 694 \times 360$ measurements and an 512×512 image to reconstruct.

Implementation available at github.com/isucsp/imgRecSrc.

Real data provided by Joe Gray, CNDE. Thanks!

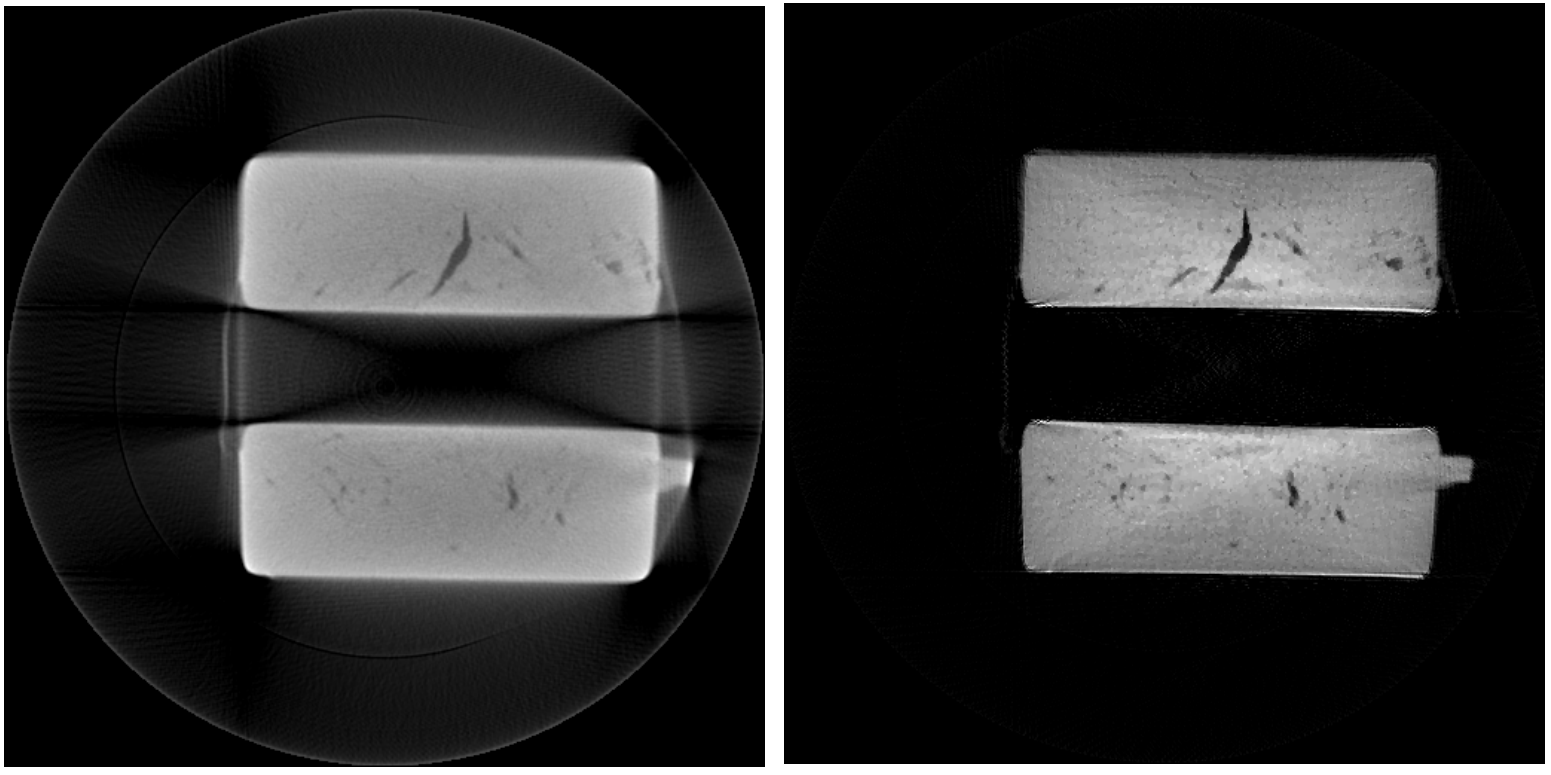

(a) FBP (b) NPG-BFGS ($u = 10^{-5}$)

Figure 14: Real X-ray CT: Full projections.

Comments

Our reconstruction eliminates

- the streaking artifacts across the air around the object,
- the cupping artifacts with high intensity along the border.

Note that the regularization constant u is tuned for the best reconstruction.

Inverse Linearization Function Estimate

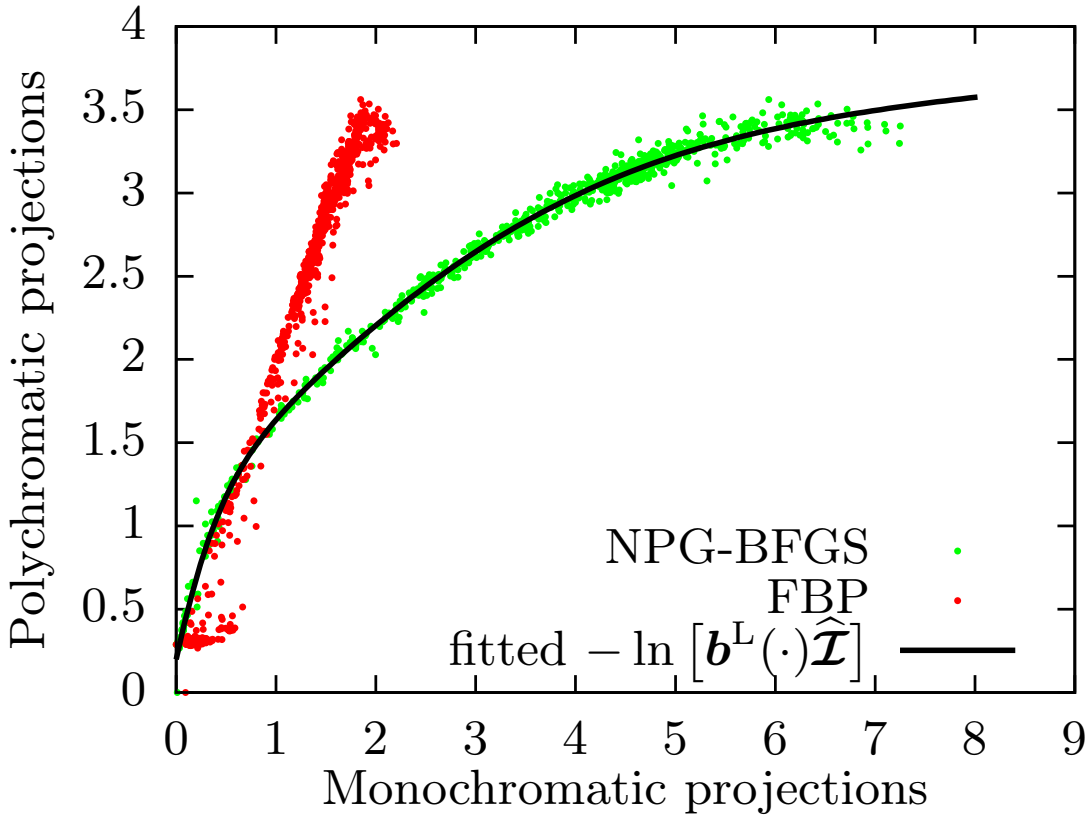

Figure 15: The polychromatic measurements as function of the monochromatic projections and its corresponding fitted curve.

residuals: large, biased for FBP; small, unbiased for NPG-BFGS, increasing variance

Real X-ray CT Example II

- X-ray source to rotation center is 8696 times of a single detector size,
- measurement array size of 1380 elements,
- projection matrix Φ constructed directly on GPU (multi-thread version on CPU is also available) with full circular mask.

yielding a nonlinear estimation problem with $N = 1380 \times 360$ measurements and an 1024×1024 image to reconstruct.

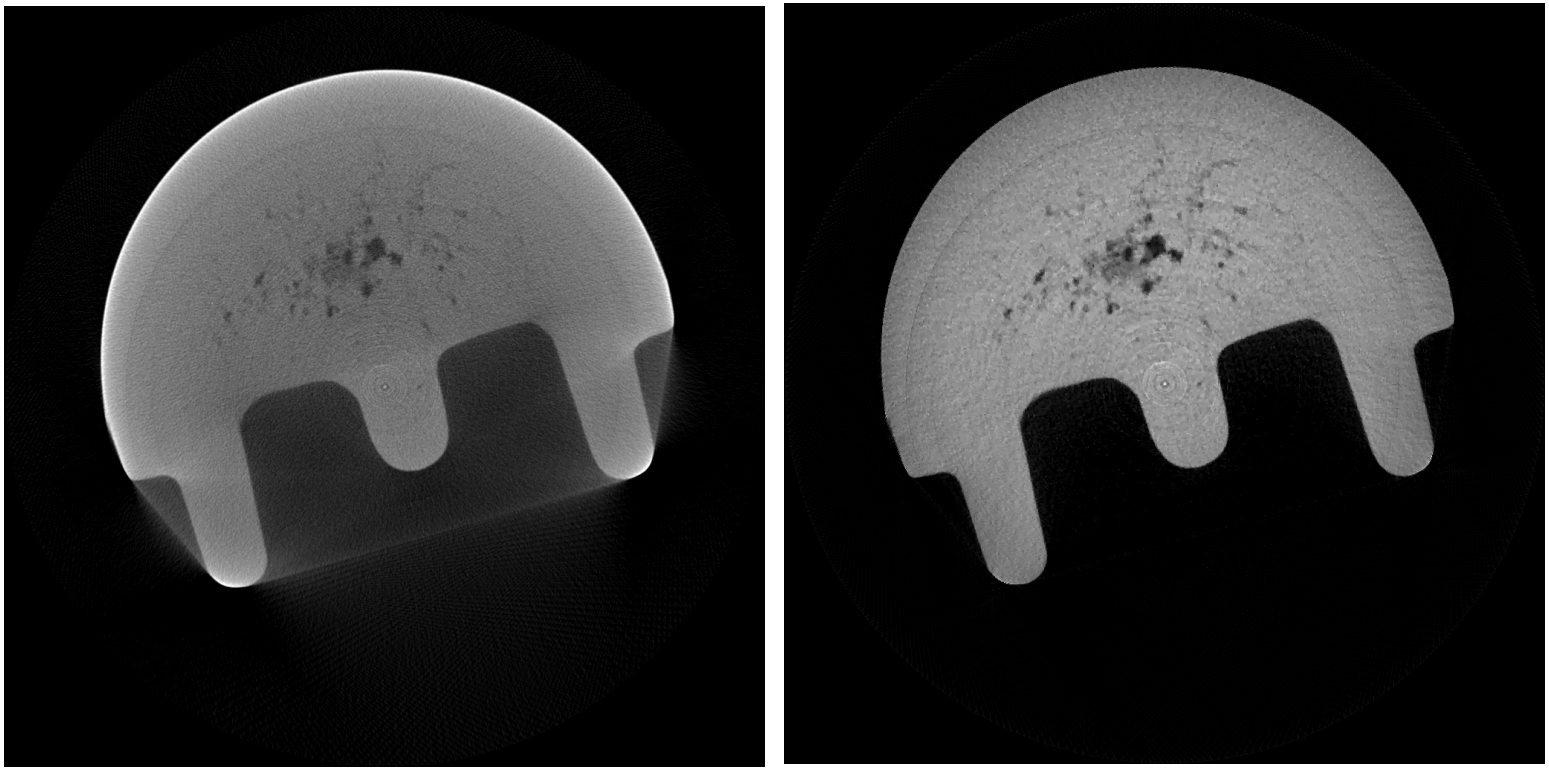

(a) FBP (b) NPG-BFGS ($u = 10^{-5}$)

Figure 16: Real X-ray CT: 360 fan-beam projections over $360°$.

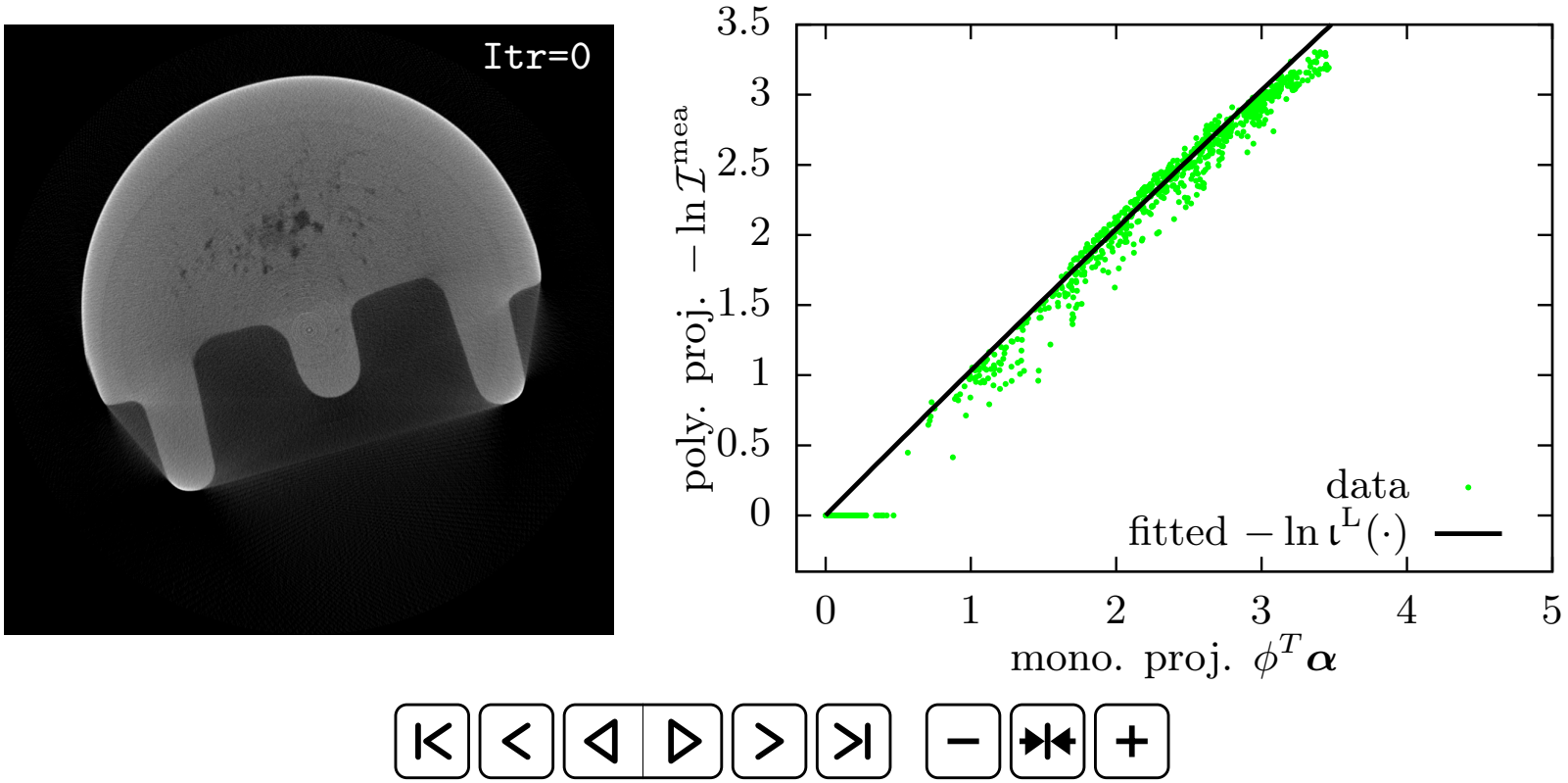

Figure 17: Estimated $\boldsymbol{x}$ and $-\ln\left(\boldsymbol{b}^{\mathrm{L}}(\cdot)\mathcal{I}\right)$ from 360 fan-beam real X-ray CT projections.

Inverse Linearization Function Estimate

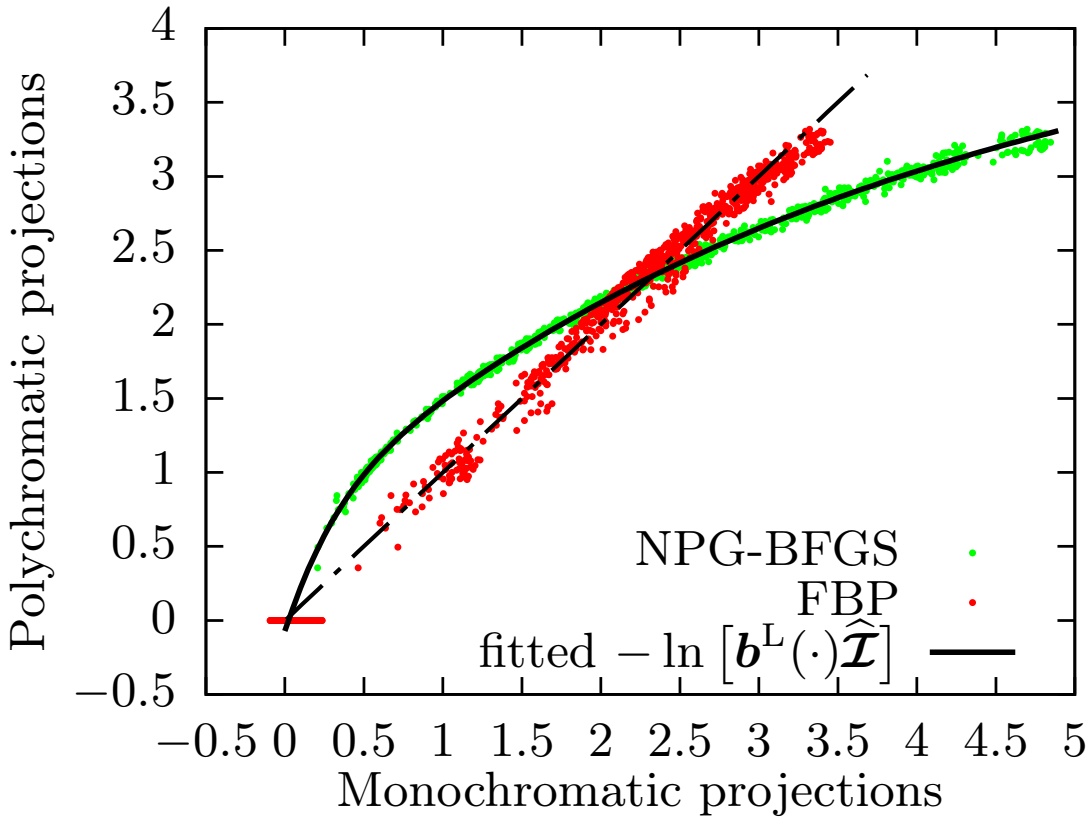

Figure 18: The polychromatic measurements as function of the monochromatic projections and its corresponding fitted curve.

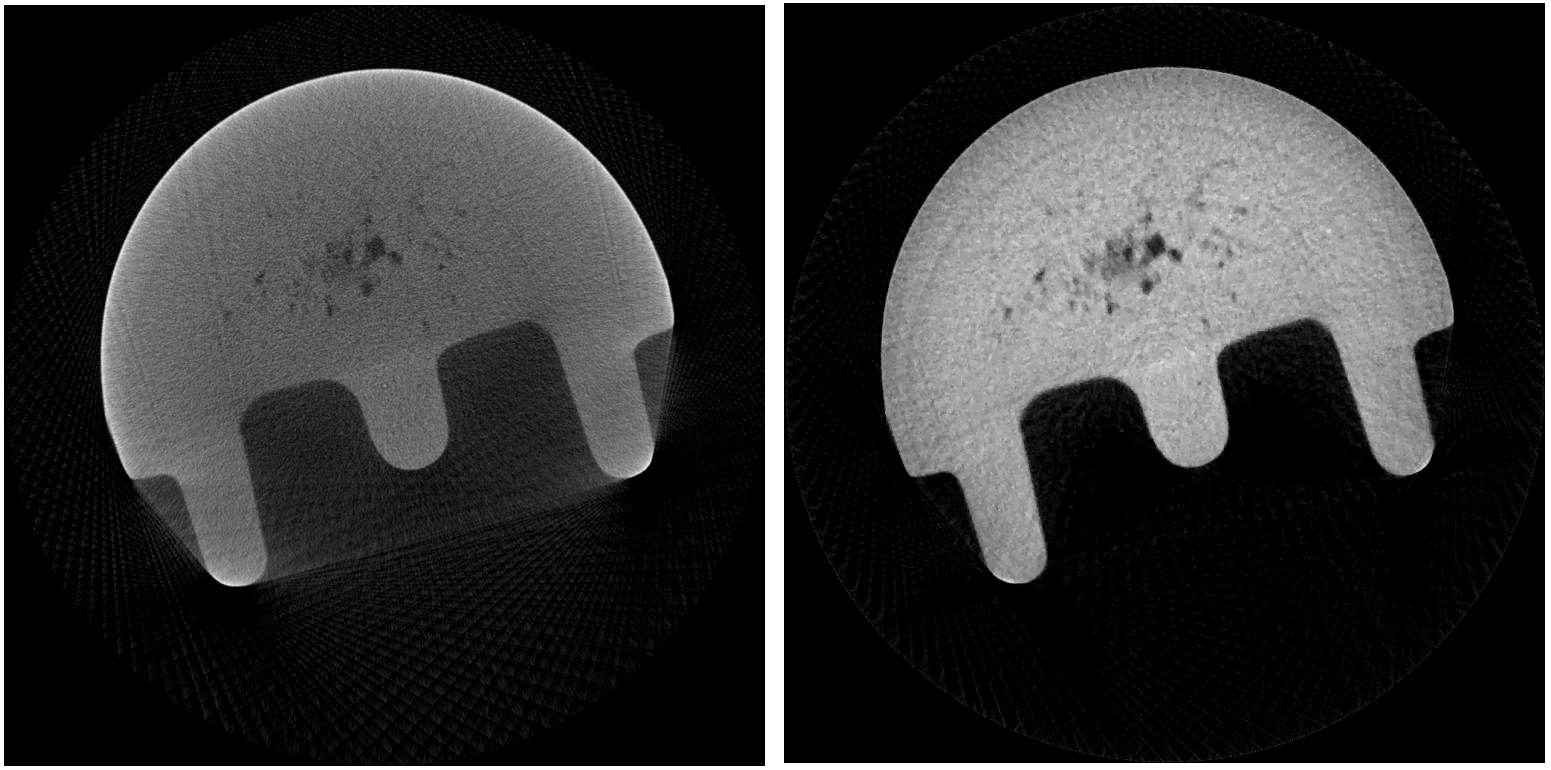

(a) FBP (b) NPG-BFGS ($u = 10^{-5}$)

Figure 19: Real X-ray CT: 120 fan-beam projections over $360°$.

Observe the aliasing artifacts in the FBP reconstruction.

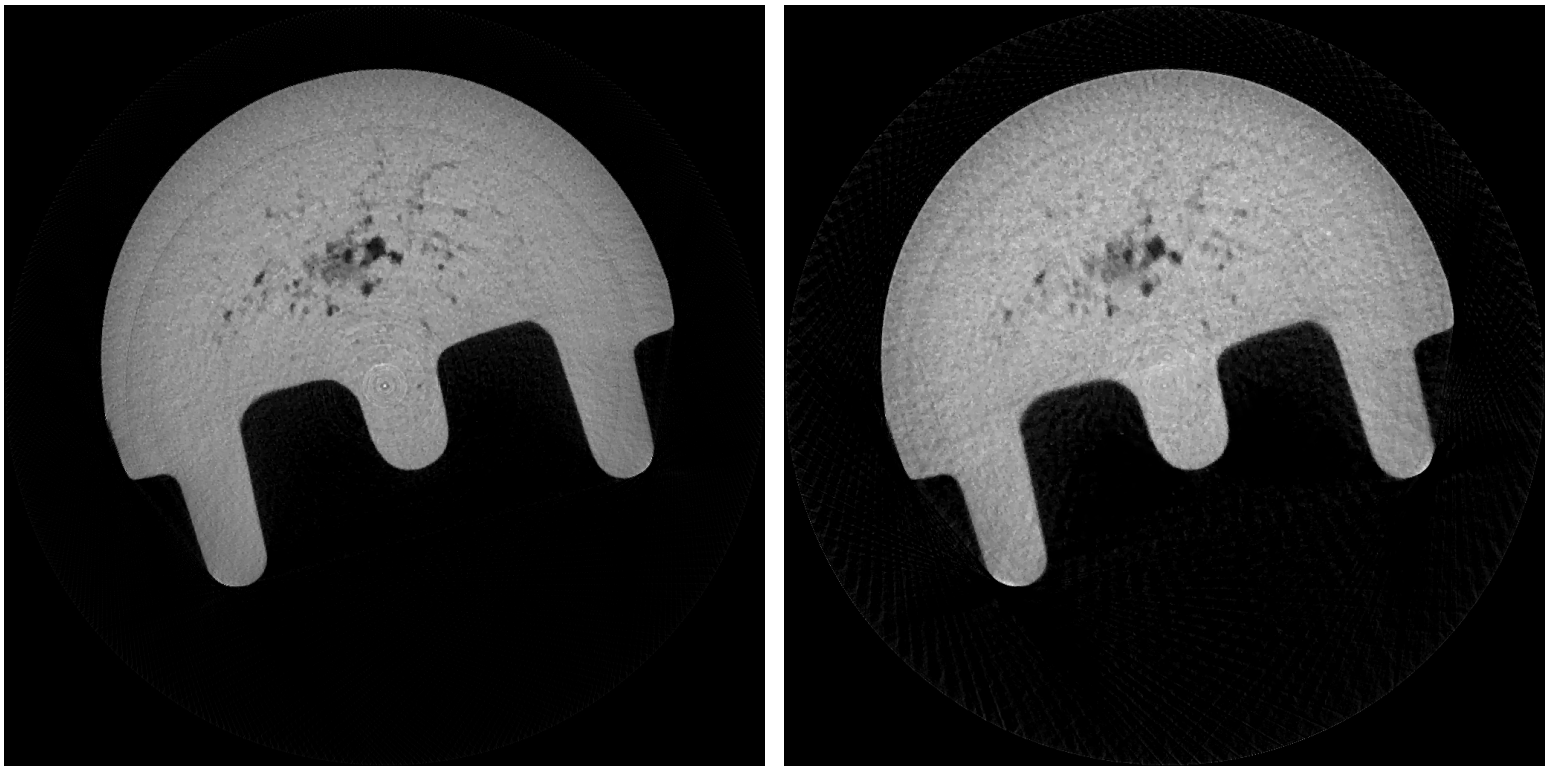

(a) 360 projections (b) 120 projections

Figure 20: NPG-BFGS ($u = 10^{-5}$) reconstructions from fan-beam projections over $360°$.

Publications

- R. G. and A. D., "Blind X-ray CT image reconstruction from polychromatic Poisson measurements," *IEEE Trans. Comput. Imag.*, vol. 2, no. 2, pp. 150–165, 2016. doi: 10.1109/tci.2016.2523431.

Conclusion

PNPG framework:

- Developed a fast framework for reconstructing signals that are sparse in a transform domain and belong to a closed convex set by employing a projected proximal-gradient scheme with Nesterov's acceleration, restart and *adaptive* step size.
- Applied the proposed framework to construct the first Nesterov-accelerated Poisson compressed-sensing reconstruction algorithm.
- Derived convergence-rate upper-bound that accounts for inexactness of the proximal operator.
- Proved convergence of iterates.
- Our PNPG approach is computationally efficient compared with the state-of-the-art.

Conclusion

Polychromatic X-ray CT:

Developed a blind method for sparse density-map image reconstruction from polychromatic X-ray CT measurements in Poisson noise.

Future work: Generalize our polychromatic signal model to handle multiple materials and develop corresponding reconstruction schemes.

References I

A. Auslender and M. Teboulle, "Interior gradient and proximal methods for convex and conic optimization," *SIAM J. Optim.*, vol. 16, no. 3, pp. 697–725, 2006.

A. Beck and M. Teboulle, "A fast iterative shrinkage-thresholding algorithm for linear inverse problems," *SIAM J. Imag. Sci.*, vol. 2, no. 1, pp. 183–202, 2009.

A. Beck and M. Teboulle, "Fast gradient-based algorithms for constrained total variation image denoising and deblurring problems," *IEEE Trans. Image Process.*, vol. 18, no. 11, pp. 2419–2434, 2009.

S. R. Becker, E. J. Candès, and M. C. Grant, "Templates for convex cone problems with applications to sparse signal recovery," *Math. Program. Comp.*, vol. 3, no. 3, pp. 165–218, 2011. [Online]. Available: `http://cvxr.com/tfocs`.

M. Bertero, P. Boccacci, G. Desiderà, and G. Vicidomini, "Image deblurring with Poisson data: From cells to galaxies," *Inverse Prob.*, vol. 25, no. 12, pp. 123006-1–123006-26, 2009.

S. Bonettini, I. Loris, F. Porta, and M. Prato, "Variable metric inexact line-search-based methods for nonsmooth optimization," *SIAM J. Optim.*, vol. 26, no. 2, pp. 891–921, 2016.

References II


S. Bonettini, F. Porta, and V. Ruggiero, "A variable metric forward-backward method with extrapolation," *SIAM J. Sci. Comput.*, vol. 38, no. 4, A2558–A2584, 2016.


R. H. Byrd, P. Lu, J. Nocedal, and C. Zhu, "A limited memory algorithm for bound constrained optimization," *SIAM J. Sci. Comput.*, vol. 16, no. 5, pp. 1190–1208, 1995.


A. Chambolle and C. Dossal, "On the convergence of the iterates of the 'fast iterative shrinkage/thresholding algorithm'," *J. Optim. Theory Appl.*, vol. 166, no. 3, pp. 968–982, 2015.


L. Condat, "A primal–dual splitting method for convex optimization involving Lipschitzian, proximable and linear composite terms," *J. Optim. Theory Appl.*, vol. 158, no. 2, pp. 460–479, 2013.


A. D., R. G., and K. Qiu, "Mask iterative hard thresholding algorithms for sparse image reconstruction of objects with known contour," *Proc. Asilomar Conf. Signals, Syst. Comput.*, Pacific Grove, CA, Nov. 2011, pp. 2111–2116.


J. A. Fessler, *Image reconstruction toolbox*, [Online]. Available: `http://www.eecs.umich.edu/~fessler/code` (visited on 08/23/2016).

References III

R. G. and A. D., "Projected Nesterov's proximal-gradient signal recovery from compressive Poisson measurements," *Proc. Asilomar Conf. Signals, Syst. Comput.*, Pacific Grove, CA, Nov. 2015, pp. 1490–1495.

R. G. and A. D., "Blind X-ray CT image reconstruction from polychromatic Poisson measurements," *IEEE Trans. Comput. Imag.*, vol. 2, no. 2, pp. 150–165, 2016.

R. G. and A. D. (Oct. 2016), Projected Nesterov's proximal-gradient algorithm for sparse signal reconstruction with a convex constraint, version 6. arXiv: 1502.02613 [stat.CO].

Z. T. Harmany, R. F. Marcia, and R. M. Willett, "This is SPIRAL-TAP: Sparse Poisson intensity reconstruction algorithms—theory and practice," *IEEE Trans. Image Process.*, vol. 21, no. 3, pp. 1084–1096, Mar. 2012.

Y. Nesterov, "A method of solving a convex programming problem with convergence rate $O(1/k^2)$," *Sov. Math. Dokl.*, vol. 27, 1983, pp. 372–376.

B. O'Donoghue and E. Candès, "Adaptive restart for accelerated gradient schemes," *Found. Comput. Math.*, vol. 15, no. 3, pp. 715–732, 2015.

J. M. Ollinger and J. A. Fessler, "Positron-emission tomography," *IEEE Signal Process. Mag.*, vol. 14, no. 1, pp. 43–55, 1997.

References IV


B. T. Polyak, "Some methods of speeding up the convergence of iteration methods," *USSR Comput. Math. Math. Phys.*, vol. 4, no. 5, pp. 1–17, 1964.


B. T. Polyak, *Introduction to Optimization*. New York: Optimization Software, 1987.


J. L. Prince and J. M. Links, *Medical Imaging Signals and Systems*, 2nd ed. Upper Saddle River, NJ: Pearson, 2015.


H. Raguet, J. Fadili, and G. Peyré, "A generalized forward-backward splitting," *SIAM J. Imag. Sci.*, vol. 6, no. 3, pp. 1199–1226, 2013.


R. T. Rockafellar, *Convex Analysis*. Princeton, NJ: Princeton Univ. Press, 1970.


S. Salzo. (May 2016), The variable metric forward-backward splitting algorithm under mild differentiability assumptions, arXiv: 1605.00952 [math.OC].


S. Villa, S. Salzo, L. Baldassarre, and A. Verri, "Accelerated and inexact forward-backward algorithms," *SIAM J. Optim.*, vol. 23, no. 3, pp. 1607–1633, 2013.


R. M. Willett, M. F. Duarte, M. A. Davenport, and R. G. Baraniuk, "Sparsity and structure in hyperspectral imaging: Sensing, reconstruction, and target detection," *IEEE Signal Process. Mag.*, vol. 31, no. 1, pp. 116–126, Jan. 2014.

References V

S. J. Wright, R. D. Nowak, and M. A. T. Figueiredo, "Sparse reconstruction by separable approximation," *IEEE Trans. Signal Process.*, vol. 57, no. 7, pp. 2479–2493, 2009.

C. Zhu, R. H. Byrd, P. Lu, and J. Nocedal, "Algorithm 778: L-BFGS-B: Fortran subroutines for large-scale bound-constrained optimization," *ACM Trans. Math. Softw.*, vol. 23, no. 4, pp. 550–560, Dec. 1997.

Adaptive Step Size

1.
   - if no step-size backtracking events or increase attempts for $\mathbb{n}$ consecutive iterations, start with a larger step size

$$\overline{\beta}^{(i)} = \frac{\beta^{(i-1)}}{\xi} \qquad \text{(increase attempt)}$$

     where $\xi \in (0, 1)$ is a *step-size adaptation parameter*;
   - otherwise start with

$$\overline{\beta}^{(i)} = \beta^{(i-1)};$$

2. (backtracking search) select

$$\beta^{(i)} = \xi^{t_i} \overline{\beta}^{(i)} \tag{1}$$

   where $t_i \geq 0$ is the smallest integer such that (1) satisfies the majorization condition (1); *backtracking event* corresponds to $t_i > 0$.
3. if $\max\left(\beta^{(i)}, \beta^{(i-1)}\right) < \overline{\beta}^{(i)}$, increase $\mathbb{n}$ by a nonnegative integer $\mathbb{m}$:

$$\mathbb{n} \leftarrow \mathbb{n} + \mathbb{m}.$$

back

Restart

Whenever $f\left(\boldsymbol{x}^{(i)}\right) > f\left(\boldsymbol{x}^{(i-1)}\right)$ or $\bar{\boldsymbol{x}}^{(i)} \in C \setminus \operatorname{dom} \mathcal{L}$, we set

$$\theta^{(i-1)} = 1 \qquad \text{(restart)}$$

and refer to this action as *function restart* (O'Donoghue and Candès 2015) or *domain restart* respectively.

back

Inner Convergence Criteria

$$\text{TV:} \quad \left\| \boldsymbol{x}^{(i,j)} - \boldsymbol{x}^{(i,j-1)} \right\|_2 \leq \eta \sqrt{\delta^{(i-1)}} \tag{2a}$$

$$\ell_1\text{:} \quad \max\left(\left\| \boldsymbol{s}^{(i,j)} - \Psi^T \boldsymbol{x}^{(i,j)} \right\|_2, \left\| \boldsymbol{s}^{(i,j)} - \boldsymbol{s}^{(i,j-1)} \right\|_2 \right)$$

$$\leq \eta \left\| \Psi^T \left(\boldsymbol{x}^{(i-1)} - \boldsymbol{x}^{(i-2)} \right) \right\|_2 \tag{2b}$$

where j is the inner-iteration index,

- $\boldsymbol{x}^{(i,j)}$ is the iterate of $\boldsymbol{x}$ in the jth inner iteration step within the ith step of the (outer) PNPG iteration, and
- $$\eta \in (0, 1)$$

  is the convergence tuning constant chosen to trade off the accuracy and speed of the inner iterations and provide sufficiently accurate solutions to the proximal mapping.

back

Definition (Inexact Proximal Operator (Villa *et al.* 2013))

We say that $\boldsymbol{x}$ is an approximation of $\operatorname{prox}_{ur}\boldsymbol{a}$ with ε-precision, denoted by

$$\boldsymbol{x} \approxeq_{\varepsilon} \operatorname{prox}_{ur}\boldsymbol{a}$$

if

$$\frac{\boldsymbol{a}-\boldsymbol{x}}{u} \in \partial_{\frac{\varepsilon^2}{2u}} r(\boldsymbol{x}).$$

Note: This definition implies

$$\|\boldsymbol{x} - \operatorname{prox}_{ur}\boldsymbol{a}\|_2^2 \leq \varepsilon^2.$$

back

Relationship with FISTA I

PNPG can be thought of as a generalized fast iterative shrinkage-thresholding algorithm (FISTA) (Beck and Teboulle 2009a) that accommodates

- convex constraints,
- more general NLLs,[¶] and (increasing) adaptive step size
  - thanks to this step-size adaptation, PNPG *does not* require Lipschitz continuity of the gradient of the NLL.

back

[¶] FISTA has been developed for the linear Gaussian model.

Relationship with FISTA II

- Need $B^{(i)}$ to derive theoretical guarantee for convergence speed of the PNPG iteration.
- In contrast with PNPG, FISTA has a non-increasing step size $\beta^{(i)}$, which allows for setting

$$B^{(i)} = 1$$

for all i:[‖]

$$\theta^{(i)} = \frac{1}{2}\left[1 + \sqrt{1 + 4\left(\theta^{(i-1)}\right)^2}\right].$$

- A simpler version of FISTA is

$$\theta^{(i)} = \frac{1}{2} + \theta^{(i-1)} = \frac{i+1}{2}$$

for $i \geq 1$, which corresponds to $(\gamma, b) = (2, 0)$.

back

[‖] Y. Nesterov, "A method of solving a convex programming problem with convergence rate $O(1/k^2)$," *Sov. Math. Dokl.*, vol. 27, 1983, pp. 372–376.

Relationship with AT

(Auslender and Teboulle 2006):

$$
\begin{aligned}
\theta^{(i)} &= \frac{1}{2}\left[1+\sqrt{1+4\left(\theta^{(i-1)}\right)^2}\right] \\
\overline{\boldsymbol{x}}^{(i)} &= \left(1-\frac{1}{\theta^{(i)}}\right)\boldsymbol{x}^{(i-1)}+\frac{1}{\theta^{(i)}}\widetilde{\boldsymbol{x}}^{(i-1)} \\
\widetilde{\boldsymbol{x}}^{(i)} &= \operatorname{prox}_{\theta^{(i)}\beta^{(i)}ur}\left(\widetilde{\boldsymbol{x}}^{(i-1)}-\theta^{(i)}\beta^{(i)}\nabla\mathcal{L}\left(\overline{\boldsymbol{x}}^{(i)}\right)\right) \\
\boldsymbol{x}^{(i)} &= \left(1-\frac{1}{\theta^{(i)}}\right)\boldsymbol{x}^{(i-1)}+\frac{1}{\theta^{(i)}}\widetilde{\boldsymbol{x}}^{(i)}
\end{aligned}
$$

Other variants with infinite memory are available at (Becker *et al.* 2011).

back

Heavy-ball Method

(Polyak 1964; Polyak 1987):

$$\boldsymbol{x}^{(i)} = \mathrm{prox}_{\beta^{(i)}ur}\left(\boldsymbol{x}^{(i-1)} - \beta^{(i)}\nabla\mathcal{L}\left(\boldsymbol{x}^{(i-1)}\right)\right) + \Theta^{(i)}\left(\boldsymbol{x}^{(i-1)} - \boldsymbol{x}^{(i-2)}\right).$$

back

Variable-metric Forward-Backward Methods: I

(Salzo 2016) (see also (Bonettini, Loris, *et al.* 2016)):

$$\begin{aligned} \boldsymbol{z}^{(i)} &= \boldsymbol{x}^{(i)} - \beta^{(i)} \big(D^{(i)}\big)^{-1} \nabla \mathcal{L}(\boldsymbol{x}^{(i)}) \\ \boldsymbol{y}^{(i)} &\triangleq \operatorname{prox}^{D^{(i)}}_{\beta^{(i)} ur}\big(\boldsymbol{z}^{(i)}\big) \\ \boldsymbol{x}^{(i+1)} &= \boldsymbol{x}^{(i)} + \lambda^{(i)} \big(\boldsymbol{y}^{(i)} - \boldsymbol{x}^{(i)}\big) \end{aligned}$$

where

$$\operatorname{prox}^{D}_{\beta ur}(\boldsymbol{z}) \triangleq \arg\min_{\boldsymbol{x}} \frac{1}{2\beta} \|\boldsymbol{x} - \boldsymbol{z}\|^2_D + ur(\boldsymbol{x}),$$

$\lambda^{(i)}$ and $\beta^{(i)}$ are the relaxation parameter and step size.
Interpretation. If we set $\lambda^{(i)} = 1$ and use line search to obtain $\beta^{(i)}$, then the resulting method can be thought as generalized PG method with scaling matrix and adaptive step size.
No acceleration!

Variable-metric Forward-Backward Methods: II

(Bonettini, Porta, *et al.* 2016):

$$\Theta^{(i)} = \left(\theta^{(i-1)} - 1\right)/\theta^{(i)}$$
$$\bar{\boldsymbol{x}}^{(i)} = P_C\left(\boldsymbol{x}^{(i-1)} + \Theta^{(i)}\left(\boldsymbol{x}^{(i-1)} - \boldsymbol{x}^{(i-2)}\right)\right)$$
$$\boldsymbol{x}^{(i)} = \mathrm{prox}^{D^{(i)}}_{\beta^{(i)}ur}\left(\bar{\boldsymbol{x}}^{(i)} - \beta^{(i)}\left(D^{(i)}\right)^{-1}\nabla\mathcal{L}\left(\bar{\boldsymbol{x}}^{(i)}\right)\right)$$

where $\theta^{(i)}$ is the solution to

$$\left(\theta^{(i-1)}\right)^2 \geq \left(\theta^{(i)}\right)^2 - \theta^{(i)}$$

and $\beta^{(i)}$ is decreasing only (no adaptation!).